

A two-stage robust optimisation for terminal traffic flow problem

K.K.H. NG^{a,b,c}, C.K.M. LEE^c, Felix T.S. CHAN^c, Chun-Hsien CHEN^{a,*}, Yichen QIN^d

^a *School of Mechanical and Aerospace Engineering, Nanyang Technological University, 50 Nanyang Avenue, Singapore 639798, Singapore*

^b *School of Electrical and Electronic Engineering, Nanyang Technological University, 50 Nanyang Avenue, Singapore 639798, Singapore*

^c *Department of Industrial and Systems Engineering, The Hong Kong Polytechnic University, Hung Hom, Hong Kong, China*

^d *School of Economics and Management, Shanghai Maritime University, Shanghai, 201306, China*

* *Corresponding author. Address School of Mechanical and Aerospace Engineering, Nanyang Technological University, North Spine (N3), Level 2, 50 Nanyang Avenue, Singapore 639798, Singapore. Tel.: +65 6790 4888; fax: +65 6792 4062.*

Email Address: kamhung.ng@ntu.edu.sg (K.K.H. NG), ckm.lee@polyu.edu.hk (C.K.M. LEE), f.chan@polyu.edu.hk (Felix T.S. CHAN), mchchen@ntu.edu.sg (C.-H. CHEN), ycqin@shmtu.edu.cn (Yichen QIN)

Acknowledgment

The authors would like to express their gratitude and appreciation to the anonymous reviewers, the editor-in-chief and the guest editors for providing valuable comments for the continuing improvement of this article. The research is supported by *School of Mechanical and Aerospace Engineering, Nanyang Technological University, Singapore, School of Electrical and Electronic Engineering, Nanyang Technological University, Singapore and the Hong Kong Polytechnic University, Hong Kong*. Our gratitude is also extended to the Research Committee and the *Department of Industrial and Systems Engineering, the Hong Kong Polytechnic University* for support of the project (RU8H). The authors would like to express their appreciation to *the Hong Kong International Airport* and *FlightGlobal* for their assistance with the data collection.

Author contributions section

K.K.H. NG: Conceptualisation, methodology, data curation, formal analysis, algorithm design, resources, writing – original draft, writing – review & editing

C.K.M. LEE: Conceptualisation, validation, resources, supervision

Felix T.S. CHAN: funding acquisition, supervision

Chun-Hsien CHEN: Conceptualisation, validation, resources, supervision, review & editing, funding acquisition

Yichen QIN: Conceptualisation, review & editing

Declarations of interest: none

1 A two-stage robust optimisation for terminal traffic flow problem

2

3 **Abstract**

4 Airport congestion witnesses potential conflicts: insufficient terminal airspace and delay propagation within
5 scrambled the competition in the terminal manoeuvring area. Re-scheduling of flights is needed in numerous
6 situations, heavy traffic in air segments, holding patterns, runway schedules and airport surface operations.
7 Robust optimisation for terminal traffic flow problem, providing a practical point of view in hedging uncertainty,
8 can leverage the adverse effect of uncertainty and schedule intervention. To avoid delay propagation throughout
9 the air traffic flow network and reduce the vulnerability to disruption, this research adopts a two-stage robust
10 optimisation approach in terminal traffic flow. It further enhances the quality of Pareto-optimality Benders-dual
11 cutting plane based on core point approximation in the second stage recourse decision. The efficiency of the
12 cutting plane algorithm is evaluated by a set of medium sized real-life scenarios. The numerical results show
13 that the proposed scheme outperforms the well-known Pareto-optimal cuts in Benders-dual method from the
14 literature.

15

16 **Keywords:** Robust optimisation; Terminal traffic flow problem; Benders cuts selection scheme; Dynamic
17 relative interior point

18

1 **1. Introduction**

2 Terminal Traffic Flow Problem (TTFP) schedules each approaching flight to its respective approaching
3 decisions, by considering the assignment and conflict avoidance of the air route, joint-segment, common guided
4 path, aeronautical holding and landing decisions [1, 2]. The complexity of the model for TTFP depends on the
5 presence of air traffic and the limited availability of airside resources [3]. The uncertainty of air traffic delay
6 may disrupt the process of scheduling and affect the reliability on predetermined optimal schedule as
7 deterministic variability can result in infeasibility for some realisations of uncertainty [2, 4-9]. Therefore, Robust
8 Optimisation (RO) deals with an optimisation problem focusing on a certain measurement on the robustness of
9 a solution against the ambiguity of the underlying distribution of the uncertain variables [10, 11].
10 Decisionmakers can analyse the robustness and estimate their affordability of the worst-case outcome. Hence,
11 the design of TTFP should needs to the robust approach to the inherent uncertainty when unanticipated delay is
12 inevitable in practical situation of Air Traffic Control (ATC) performance [12, 13].

13 Of the few recent relevant papers that have considered uncertainty in TTFP, the most recent publications
14 have considered the deterministic and stochastic approaches for Aircraft Sequencing and Scheduling Problem
15 (ASSP) [1]. One primary objective of ASSP is to maintain smooth runway scheduling and sufficient separation
16 time to alleviate the hazard effect of wake-vortex during the approaching and departing procedures [14].
17 Imposing the separation time requirement between adjacent flights, which is the standard ATC regulation in
18 civil aviation, can result in fatal accidents and uncommon operations [15-17]. The category-based minimal
19 separation requirement is a sequence parameter that includes buffer time between adjacent flights to ensure safe
20 ATC [6, 18, 19]. Readers can refer to the variants of the deterministic ASSP model from the survey paper [1] or
21 through following literature (E.g., Aircraft Landing Problem (ALP) [12, 20-26], Aircraft Take-off Problem (ATP)
22 [16, 23], ASSP with mixed-mode operations [6, 27, 28], and ASSP with runway configuration switch [29-32]).

23 Coordination between runway scheduling and other terminal traffic flow resources can also help reduce
24 the problem of airport congestion [33]. The major challenge in managing air traffic flow in operations research
25 is the complex coordination of all the interconnected air and surface traffic flow resources in mathematical
26 modelling [1]. [Jacquillat and Odoni \[33\]](#) explained that joint optimisation for interdependent activities can
27 mitigate airport congestion via scheduling interventions at the strategic level. Various applications can be
28 considered joint decisions on airport surface traffic operations, such as runway scheduling and taxiway
29 optimisation [34, 35] and runway configuration design and ASSP scheduling [30]. Comparatively, TTFP
30 considers the resource coordination of ATC resources close to the Terminal Manoeuvring Area (TMA). [Samà,
31 D'Ariano, D'Ariano and Pacciarelli \[36\]](#) proposed an alternative graph method using a network graph
32 considering all the ATC resources in TMA. The re-routing strategies for TTFP using the alternative graph
33 method can redirect flights to other approaching paths according to the on-going traffic congestion level [37-
34 39]. [Tian, Wan, Han and Ye \[40\]](#) proposed a terminal resource allocation model considering the emission and
35 noise impact in congested terminal airspace configuration. [Corolli, Lulli, Ntamo and Venkatachalam \[41\]](#)
36 proposed a heuristic approach to solve the TTFP model with ground holding, airborne holding and rerouting
37 against the stochastic factor of weather in a terminal airspace. The state-of-the-art literature on TTFP focuses

1 on the fault-driven re-scheduling method and stochastic optimisation instead of RO approach.

2 RO is a relatively new research area for decision making over a postulated or user specific uncertainty set
3 [42-44]. It was first introduced by [Daniels and Kouvelis \[45\]](#), and various publications have contributed to the
4 research field in different research domain, including finance [46], energy [47, 48], human resource [49],
5 machine scheduling [50], health services [51], network resilience [52, 53] and transportation engineering [53-
6 55]. The RO provides a solution that is feasible over a set of worst-case scenarios [6, 43, 56, 57]. The motivation
7 to use robust criterion in real-world engineering applications ensures that the solution compensates for the
8 known risk when wrong decisions impose considerable adverse effects on the solution quality [10, 58-62]. Since
9 flight delays and airport congestion are frequently occur, the adoption of robust criterion will neutralise the
10 possible delay propagation by considering the ambiguity of the underlying distribution of unknown parameters
11 [60, 63-65].

12 A robust nonlinear optimisation problem with a convex function and linear constraints with polyhedral
13 uncertainty set can be reformulated by applying the duality theory [66, 67] or via data mining technique [68].
14 The optimisation methods for RO depend on the class of the problem and the domain of the uncertainty set [69].
15 [Gorissen, Yanikoğlu and den Hertog \[70\]](#) and [Yanikoğlu, Gorissen and den Hertog \[71\]](#) provide general
16 guidelines for the RO approach. The practical difficulty in solving a nonlinear RO problem may be due to the
17 nature of the min-max or the max-min structure. This leads to an investigation of a two-stage RO approach by
18 its robust counterpart in exploiting the deterministic equivalent in the nonlinear RO problem. In the two-stage
19 RO approach, the first-stage attempts to solve the problem with deterministic variables, while the robust
20 counterpart of the second stage computes the decision over the worst-case scenario and develops a cutting-plane
21 method to achieve computational tractability in solving the two-stage RO. Readers can refer to the introduction
22 of the robust counterpart corresponding to the uncertainty region [43, 70, 71].

23 Benders-dual cutting plane method is used to generate cutting planes on the respective dual form problem
24 involving continuous variables. Valid cutting planes guarantees convergence of the two-stage RO approach by
25 periodically solving the first-stage and second-stage problems. [Lei, Lin and Miao \[72\]](#) presented a multiple-
26 optimality cutting scheme to reduce the number of iterations required and get faster convergence in the two-
27 stage RO approach. [Rahmaniani, Crainic, Gendreau and Rei \[73\]](#) suggested several methods to accelerate the
28 convergence speed of the decomposition algorithm. In the two-stage RO approach, solving RO problems in a
29 decomposition framework to find the worst-case scenarios can be computationally expensive. Furthermore, the
30 number of valid cuts is associated with the number of iterations required to solve the two-stage RO approach.
31 Therefore, generating a stronger cutting plane or multi-cutting plane could strengthen the convergence of the
32 two-stage RO approach. [Magnanti and Simpson \[74\]](#) and [Magnanti and Wong \[75\]](#) investigated the degeneracy
33 of the sub-problems, and found cuts from multiple optimal solutions can have different strengths. [Magnanti and
34 Wong \[75\]](#) proposed a cut-selection scheme by an auxiliary optimisation problem to generate Pareto-optimal
35 cuts. [Magnanti and Wong \[75\]](#) method attempted to generate a Pareto-optimal cut that could dominate other
36 possible cuts in the dual problem. The estimation of the Pareto-optimal solution can be generated from a relative

1 interior point from the initial solution of the first-stage problem. However, solving the auxiliary optimisation
2 problem can be time-consuming and numerically instable [73]. [Papadakos \[76\]](#) further improved the
3 convergence of the [Magnanti and Wong \[75\]](#) method by algorithm modification. Their method successfully
4 disregarded the equality constraint that illustrated the dependency on the optimal solution from the second-stage
5 problem and introduced a convex combination of initial and incumbent core points. In their numerical analysis,
6 the value of λ of the convex combination of the initial and incumbent core points is considered 0.5. [de Sá, de
7 Camargo and de Miranda \[77\]](#) pointed out that fixing this λ value during the iterative procedure of two-stage
8 optimisation may not be appropriate and that the possibility of finding the Pareto-optimal cuts is subjected to
9 the quality of the core point approximation. In their approach, [de Sá, de Camargo and de Miranda \[77\]](#)
10 considered the ratio of the convex combination as an optimisation problem when unbounded situation in the
11 second-stage optimisation problem was encountered. The aforementioned approaches considered the static core
12 point or estimated the core point by the optimisation method.

13 There is no perfect way to obtain the best core point as the evaluation of the effectiveness of a Pareto-
14 optimal cut and the quality of the core point requires a post-hoc analysis. Obtaining the best core point is
15 challenging in the two-stage RO approach. [de Sá, de Camargo and de Miranda \[77\]](#) method gives an idea of the
16 dynamic core point, however, it can change the λ value of the convex combination when solving the second-
17 stage problem, which is infeasible. Furthermore, [de Sá, de Camargo and de Miranda \[77\]](#) method may not be
18 effective if the first and second- stage problems are always feasible during the iterative procedure. The proposed
19 approach ensures core-point estimation is limited to the infeasibility in the second-stage optimisation problem,
20 but relative to the ‘information’ of the iterative procedure of the two-stage RO approach. It further improves the
21 convergence of [Papadakos \[76\]](#) method by considering dynamic core points. To yield a relatively high quality
22 of Pareto-optimal cuts, the characteristics of the core point approximation by a stochastic element and the
23 association of the convergence performance can enhance the convergence speed of the two-stage RO approach,
24 as finding the best core point at each iteration is computationally difficult. The strength of the Benders-dual
25 cutting plane can be closely related to the convergence process of the incumbent lower bound value. We believe
26 that several unchanged lower bound values in the iterative procedure can be an ‘alert’ of a poor incumbent
27 relative interior point. Therefore, we suggest a meta-heuristic approach as an adaptive parameter to work on the
28 convergence procedure of the two-stage RO approach. To the best of our knowledge, the dynamic core point by
29 the meta-heuristic for the two-stage RO approach is not covered by the literature.

30 The computational efficiency can further be enhanced by the recent advancement of optimisation methods,
31 such as meta-heuristics, which does not guarantee to find an optimum solution; however, it can effectively
32 obtain a near-optimal that satisfies the needs for commercial engineering applications [1, 78, 79]. Please note
33 that in the proposed approach, the convergence procedure is guided by a two-stage RO approach and a Benders-
34 dual cutting plane. A meta-heuristic worked as an adaptive parameter in the two-stage RO approach. Therefore,
35 the proposed approach can reach an optimal solution, however, the speed of convergence is subjected to the
36 performance of the meta-heuristics and the strength of the Pareto-optimal cuts.

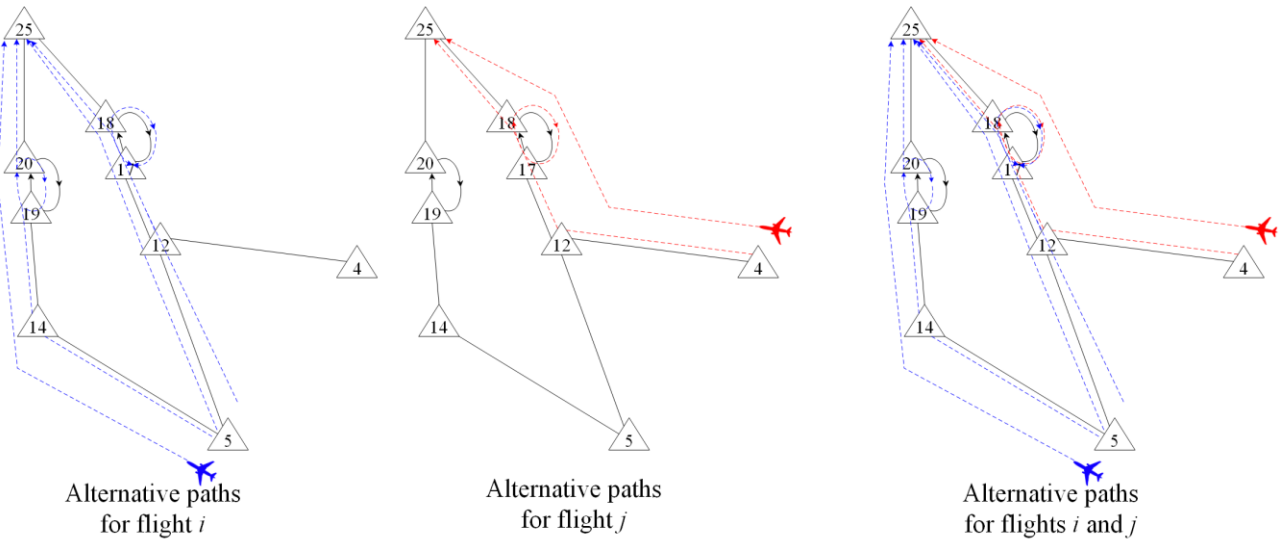
1 This work introduced a two-stage RO approach for TTFP and proposed dynamic core-point estimation
2 based on meta-heuristics. First, an alternative path method for TTFP was proposed. The alternative graph
3 method proposed by [Samà, D’Ariano, D’Ariano and Pacciarelli \[36\]](#) considers disjunctive graphs to represent
4 the traverse operations of TMA resources from entry waypoints to runways for all flights. Comparatively, path
5 selection using Directed Acyclic Graph (DAG), which is a directed graph with no directed cycles [\[80, 81\]](#), in
6 an alternative path method is considered since each flight has a limited number of choices of alternative paths
7 when approaching. Therefore, an alternative path method for TTFP is suggested. Second, a min-max TTFP with
8 uncertainty is introduced. Intuitively, the flight time between TMA resources is uncertain and subject to minor
9 perturbations of dynamic changes in wind speed, weather conditions and current traffic conditions. The
10 addressed imprecision of flight time due to the disturbance in flight speed and wind direction is practical in
11 common operations. The nonlinear Robust TTFP is reformulated as a two-stage problem with a structure of
12 mixed-integer linear programming. Therefore, the model is tractable using the MILP solver. Third, we proposed
13 a parameter to determine core-point approximation via meta-heuristic and enhance the computational efficiency
14 based on [Papadakos \[76\]](#) auxiliary optimisation problem. [de Sá, de Camargo and de Miranda \[77\]](#) method
15 suggests a formulation of core point approximation to adjust the core point when the second-stage recourse
16 decision is unbounded. Our proposed method is inspired by [de Sá, de Camargo and de Miranda \[77\]’s](#) work and
17 considers a dynamic core point estimation associated with the convergence performance of the two-stage RO
18 approach. Core algorithmic components from Simulated Annealing (SA) are extracted and integrated with the
19 two-stage RO approach. The proposed two-stage RO approach incorporates the synergy of Benders-dual cutting
20 plane, Pareto-optimality and core point approximation by meta-heuristics in an interdependent and interaction-
21 based algorithm framework that provides a high practical efficacy on better convergence properties in solving
22 an two-stage RO problem.

23 After providing a short summary of the research, the contemporary research development and in-depth
24 literature review on ASSP, TTFP, the two-stage RO approach and the cutting plane methods are presented in
25 **Section 1. Section 2** illustrates the problem background and the mathematical formulation of TTFP. **Section 3**
26 presents the two-stage RO approach for TTFP by realising the worst-case scenarios. **Section 4** introduces the
27 Benders-dual cutting plane and the two common Pareto-optimal cutting plane schemes. The proposed core point
28 approximation via meta-heuristic and Pareto-optimal cutting plane using the dynamic core point method are
29 presented in the same Section. **Section 5** evaluates the Pareto-efficiency of the proposed cutting plane method
30 by solving the medium-sized instances based on real-life flight data. The concluding remarks and limitations
31 are presented in **Section 6**.

32 **2. Terminal traffic flow problem**

33 The deterministic terminal traffic flow problem is illustrated herein with some of its basic properties. We
34 have considered an alternative path planning in TMA, where the set of paths are pre-generated and each
35 approaching flight is assigned to a path from its entry waypoints to the runway. The path assignment for each
36 flight needs to be determined in the scheduling decision, given the hard constraints of sufficient longitudinal
37

1 separation between flights and conflict-free approaching in TTFP. The proposed model makes several
 2 assumptions. First, the air routes near the TMA within the decision horizon are fixed. The set of alternative paths
 3 and landing directions may vary from time to time due to changes in wind direction and the degree of the
 4 headwind. This assumption can be realised by considering a time-variant alternative path model. Second, an
 5 actual operation is assumed to be free from operational failures, such as missed approach, emergency landing,
 6 engine failure and abnormal operations. Third, we assume the imprecise estimation of flight time on air route
 7 falls into an interval case in RO. Fourth, mono-aeronautical holding for each racetrack is sufficient in our case
 8 study for an airport as some approaching paths have several racetracks and the sufficient capacity to handle
 9 daily traffic.



10
11 **Fig. 1.** A schematic diagram of alternative paths model (a toy problem)

12 For ease of explanation, we have presented a schematic diagram of an alternative path model using a toy
 13 problem in **Fig. 1**, where flights j and i will be approaching from entry waypoint 5 and towards destination
 14 waypoint 25. An approaching route is usually presented in the form of a directed graph. Therefore, there are a
 15 limited number of approaching paths. **Fig. 1** indicates alternative paths $\{4, 12, 17, 25\}$ and $\{4, 12, 17, 18, 25\}$
 16 for flight j (middle one in **Fig. 1**) and alternative paths $\{5, 14, 19, 25\}$, $\{5, 14, 19, 20, 25\}$, $\{5, 12, 17, 25\}$ and
 17 $\{5, 12, 17, 18, 25\}$ for flight i (left one in **Fig. 1**). The terminal traffic flow model attempts to determine the
 18 best and conflict-free solution with respect to the objective function. The joint decision requires checking if
 19 there is any conflict or violation of the constraints regarding the selected paths for flights j and i from a set of
 20 alternative paths (right one in **Fig. 1**). For Instance, if flight i takes $\{5, 12, 17, 25\}$ and flight j takes $\{4, 12,$
 21 $17, 18, 25\}$ as their approaching route, respectively, then the solution must satisfy non-overtaking and sufficient
 22 longitudinal separation constraints on waypoints $\{12, 17, 18, 25\}$.

23 The mathematical model of TTFP takes the following input data. The TTFP contains a terminal traffic
 24 network with multiple entry points and one landing runway in accordance with the setting of case airport and
 25 the number of $|I|$ flights to be landed in the decision horizon. Let I be the set of flights and let each flight be
 26 indexed by j, i . In ATC regulation, each pair of adjacent flights (flight j and flight i) must satisfy the minimum

1 longitudinal separation requirement δ_{ji} (in nautical miles), which is a hard constraint to accommodate the
 2 adverse effect of wake vortices generated by the leading flight. Each flight is only associated with one entry
 3 waypoint u_i^s in the decision horizon. The destination node (runway) is denoted by u_i^e . The transit node is
 4 indexed by $u, v, \pi \in V$. Since the entry waypoint is fixed in accordance with the en-route of the departure airport,
 5 the entry waypoint is a flight-specific entry waypoint parameter.

6 The model for TTFP is formulated using a directed graph $G = (V, E)$ with a set of nodes (or waypoint) V
 7 and a set of arcs E . Each path p_i contains a set of waypoints $p_i = (o, u_i^s, \dots, u_i^e, d)$ from the origin node u_i^s
 8 (more specifically, the entry waypoint) to the destination node u_i^e (more specifically, the runway). Dummy
 9 nodes o and d are introduced for the first and final nodes in the di-graph. Hence, the pair of origin and
 10 destination nodes (u_i^s, u_i^e) indicates the predetermined entry waypoint and runway in the TTFP, respectively.
 11 Edge $(u, v) \in E$ presents the flight path between two adjacent waypoints in the problem. The collection of all
 12 waypoints for a set of alternative paths P_i is indicated by $V_i^{p_i} \subset V$, whereas the set of flight paths $E_i^{p_i} \subset E$
 13 illustrates all air routes to reach the runway by using path p_i . The number of alternative paths P_i depends on
 14 the valid paths from start to end positions. Therefore, the set of nodes in the alternative path for flight i is $V_i =$
 15 $\cup_{p_i \in P_i} V_i^{p_i}$, while the set of arc in the alternative path model is $E_i = \cup_{p_i \in P_i} E_i^{p_i}$. In this regard, $V_j, V_i \in$
 16 $V, E_j, E_i \in E$ in digraph G . For the set of alternative paths P_i , we consider mono-aeronautical holding for each
 17 racetrack by introducing the artificial node on the entry/exit of the aeronautical holding racetrack.

18 Alternative paths P_i are a predefined set as the pair of origin and destination nodes (u_i^s, u_i^e) is the input
 19 of the model. For such a network, each flight is assigned with an approaching path p_i by the ATC and follows
 20 the set of waypoints to reach the destination node. A feasible schedule X is constructed by $\varphi_i^{p_i}$ and z_{jiu} . The
 21 arrival time of the destination node is a joint decision of $\varphi_i^{p_i}$ and z_{jiu} .

22

23 We use $\varphi_i^{p_i}$ as a binary decision variable for path selection.

$$24 \quad \varphi_i^{p_i} = \begin{cases} 1, & \text{if flight } i \in I \text{ is assigned to the path } p_i \in P_i. \\ 0, & \text{otherwise.} \end{cases}$$

25 z_{jiu} is a binary decision variable that is used to determine the sequence of the schedule.

$$26 \quad z_{jiu} = \begin{cases} 1, & \text{if flight } j \text{ is before flight } i \text{ on waypoint } u \text{ (not necessary immediately).} \\ 0, & \text{otherwise.} \end{cases}$$

27

28 The estimated time of arrival on entry waypoint u_i^s for flight $i \in I$ is defined as T_i and flight time from
 29 nodes u to v for flight i by $t_{i(u,v)}$. Therefore, the model measure the arrival time $\tau_{iu}^{p_i}$ on each waypoint in the
 30 path p_i for flight i regarding the choice of paths. The arrival time of node u by path p_i for flight i is denoted
 31 as $\tau_{iu}^{p_i}$, where $\tau_{iu}^{p_i} \geq 0$.

32 The main purpose of the model is to serve all arrival flights at the lowest time possible. Regarding the
 33 objective of the model, we are concerned about the path selection associated with $w_i^{p_i}$ and the completion time

1 of severing all flights C in the decision horizon. Imposing a weight $w_i^{p_i}$ for path p_i is practical, in the sense
2 that ATC and airlines wish to minimise the time for airborne holding. The weight parameter $w_i^{p_i}$ can be simply
3 defined as the number of aeronautical holding racetracks on path p_i . Indeed, additional aeronautical holding
4 may increase or take the same completion time to serve all the flights in the decision horizon. The minimisation
5 of the total number of aeronautical holdings in a solution may not offer practical meaning to the mathematical
6 model, as the optimal solution with an objective function of minimising the completion time of serving all flights
7 C implicitly implies a solution with minimum number of aeronautical holding. However, it allows a good
8 estimation of initial solution on the joint decision of $\varphi_i^{p_i}$ and z_{jiu} in the two-stage RO (will be discussed in the
9 next section). The pair (u_i^s, u_i^e) is fixed, and the decision variable $\varphi_i^{p_i}$ decides the path selection p_i from a set
10 of valid alternative paths P_i . Each path is associated with a weight coefficient $w_i^{p_i}$. We simply assume the
11 number of aeronautical holdings on p_i for the value of $w_i^{p_i}$. The decision variables z_{jiu} indicate the sequential
12 relationship for flights j and i on the waypoint u . Therefore, a feasible schedule X is the joint decision of $\varphi_i^{p_i}$,
13 z_{jiu} , $\tau_{iu}^{p_i}$ and C . A summary of the notations is presented in **Table 1**.

14
15 **Table 1**

16 Notations and decision variables.

Sets with indices	Explanation
I	A set of approaching flights in the decision horizon (index i, j)
P_i	A set of alternative paths (index p_i)
V	A vertex set of waypoints in the TMA (index $o, u_i^s, u, v, \pi, u_i^e, d$)
E	An edge set of air route in TMA
G	A directed graph consisting of a nonempty vertex set of waypoints V and an edge set of air route E in TMA
Ω	The uncertainty set
Parameters	Explanation
i, j	Flight ID $i, j \in I$
u, v, π	Transit node $u, v, \pi \in V$
o, d	The artificial node representing the start and end node $o, d \in V$
u_i^s	The entry waypoint for flight i , $u_i^s \in V$
u_i^e	The approaching runway for flight i , $u_i^e \in V$
T_i	Estimated time of arrival in the terminal control area for flight $i \in I$
$w_i^{p_i}$	The weight coefficient associated with the path selection $p_i \in P_i$
M	Large artificial variable
$t_{i(u,v)}$	The flight time from nodes u to v for flight i
δ_{ji}	Longitudinal separation time on air route between flight j and i
p_i	A path with a set of waypoints from entry waypoints u_i^s to runway u_i^e for flight $i \in I$, $p_i \in P_i$
Decision variables	Explanation
X	A solution X is constructed by $\varphi_i^{p_i}$ and z_{jiu}
$\varphi_i^{p_i}$	1, if flight i is assigned to the path p_i ; 0, otherwise
z_{jiu}	1, if flight j is before flight i on node u (not necessary immediately); 0, otherwise

$\tau_{iu}^{p_i}$	The arrival time on node u using path p_i for flight i , $\tau_{iu}^{p_i} \geq 0$
C	The completion time of the terminal traffic flow model, $C \geq 0$

1

2 2.1. Nominal problem formulation

3 Given the above notations for parameters and decision variables, we presented the nominal formulation of
4 TTFP and assumed all parameters to be deterministic. The Objective function (1) minimises the weighted
5 penalties of path assignment and the realised completion time on serving all arriving flights.

6

$$\min \sum_{i \in I} \sum_{p_i \in P_i} w_i^{p_i} \varphi_i^{p_i} + C \quad (1)$$

s. t. Constraints (2) – (13)

7

8 *Alternative paths constraints*

$$\sum_{p_i \in P_i} \varphi_i^{p_i} = 1, \forall i \in I \quad (2)$$

$$z_{jiu} + z_{iju} \leq 1, \forall i, j \in I, i < j, \forall u \in V_j \cap V_i \quad (3)$$

$$\varphi_i^{p_i} + \varphi_j^{p_j} \leq z_{jiu} + z_{iju} + 1, \forall i, j \in I, i \neq j, \forall u \in V_j \cap V_i, \forall p_i \in P_i, \forall p_j \in P_j \quad (4)$$

$$z_{ijv} - z_{iju} \geq \sum_{p_i \in P_i} \varphi_i^{p_i} + \sum_{p_j \in P_j} \varphi_j^{p_j} - 2, \forall j, i \in I, j \neq i, \forall (u, v) \in E_j \cap E_i \setminus \{(o, u_i^s), (u_i^e, d)\} \quad (5)$$

9

10 Each flight must assign an approaching path p_i from a set of alternative paths P_i using decision variables
11 $\varphi_i^{p_i}$ in Constraint set (2). Constraint set (3) explains a sequential relationship using decision variable z_{jiu} . If
12 the assigned paths for flights j and i contain node u , then flight j must pass through node u either earlier or
13 later than flight i . Constraint set (4) illustrates the association of decision variables $\varphi_i^{p_i}$ and z_{jiu} . Constraints
14 (5) describe the overtaking constraints of any pair of flights j and i .

14

15 *Constraints of arrival time at waypoints and separation time requirements*

$$\tau_{io}^{p_i} \geq T_i \varphi_i^{p_i}, \forall i \in I, \forall p_i \in P_i \quad (6)$$

$$\tau_{iu}^{p_i} \leq M \varphi_i^{p_i}, \forall i \in I, \forall u \in P_i \quad (7)$$

$$C - \tau_{id}^{p_i} \geq 0, \forall i \in I, \forall p_i \in P_i \quad (8)$$

$$\tau_{iv}^{p_i} - \tau_{iu}^{p_i} \geq t_{i(u,v)} - M(1 - \varphi_i^{p_i}), \forall i \in I, \forall p_i \in P_i, \forall (u, v) \in E_i, u < v \quad (9)$$

$$\sum_{\substack{p_i \in P_i \\ u \in V_i^p}} \tau_{iu}^{p_i} - \sum_{\substack{p_j \in P_j \\ u \in V_j^p}} \tau_{ju}^{p_j} \geq \delta_{ji} - M(1 - z_{jiu}), \forall i, j \in I, i \neq j, \forall u \in V_j \cap V_i \setminus \{o, d\} \quad (10)$$

16

17 The arrival time of the entry route is represented by the first dummy node o ; $\tau_{io}^{p_i}$ indicates the ready time
for TTFP using path p_i for all flights $i \in I$ by Constraint set (6). Constraint set (7) explains that the arrival

1 time $\tau_{iu}^{p_i}$ for all nodes $u \in P_i$ is positive when p_i is selected. Otherwise, $\tau_{iu}^{p_i}$ is zero. $\tau_{id}^{p_i}$ indicates the arrival
2 time on runway for flight i using path p_i . The completion time C on serving all arrival flights is calculated by
3 Constraints set (8) and must be larger than or equal to $\tau_{id}^{p_i}$. The flight time $t_{i(u,v)}$ from node u to node v is
4 computed using Constraint set (9). Depending on the path selection by $p_j \in P_j$ and $p_i \in P_i$ and any union of
5 node $u \in V_j \cap V_i \setminus \{o, d\}$, Constraint set (10) enforces the arrival time on node u by flights j and i that need
6 to satisfy the longitudinal separation requirement δ_{ji} .

7

8 *Number sets of decision variables*

$$\varphi_i^{p_i} \in \{0,1\}, \forall i \in I, \forall p_i \in P_i \quad (11)$$

$$z_{jiu} \in \{0,1\}, \forall j, i \in I, j \neq i, \forall u \in V_j \cap V_i \quad (12)$$

$$\tau_{iu}^{p_i} \in \mathbb{R}^+, \forall i \in I, \forall p_i \in P_i, \forall o, u, d \in P_i \quad (13)$$

9 The decision variables $\varphi_i^{p_i}$ and z_{jiu} are binary variables in nature, as explained by the Constraints (11)
10 and (12). Constraint set (13) indicates that $\tau_{iu}^{p_i}$ is a positive real number.

11

12 3. Formulation of the two-stage robust terminal traffic flow problem

13 The nominal model can be solved as a mixed-integer linear program given all the parameters are known.
14 However, the disturbance in flight speed, head wind speed and delay in air traffic can affect the actual flight
15 time from the entry waypoints to the runway. The solution obtained by the nominal model may not be
16 appropriate as the uncertainty factor can lead to violation of the longitudinal separation requirement. To address
17 the uncertain factor $\tilde{t}_{i(u,v)}$, we reformulate TTFP by adopting the two-stage RO approach with Bertsimas-Sim
18 uncertainty. We first introduce the postulated uncertainty set in this work, and further explain the two-stage RO
19 approach for TTFP. In the two-stage RO framework, the first-stage is to determine path selection, and the
20 second-stage to determine completion time of serving all arrival flights under the worst-case scenarios.

21

22 3.1. Definition of uncertainty set

23 In this section, we present the description of uncertainty set for TTFP. The flight time on air route $\tilde{t}_{i(u,v)}$
24 falls under an interval $[\underline{t}_{i(u,v)}, \bar{t}_{i(u,v)}]$, where $\underline{t}_{i(u,v)} \leq \bar{t}_{i(u,v)}$, with respect to the minimum and maximum flight
25 times on edge $(u, v) \in E_i$ for flight $i \in I$. The uncertainty set is defined by Ω in Equation (14).

26

$$\Omega = \left\{ \tilde{t}_{i(u,v)}, \forall i \in I, \forall (u, v) \in E_i: \tilde{t}_{i(u,v)} = \underline{t}_{i(u,v)} + \hat{t}_{i(u,v)} \theta_{i(u,v)}^{p_i}, \theta_{i(u,v)}^{p_i} \in \{0,1\} \right\} \quad (14)$$

27

28 The arbitrary uncertainty set Ω is finite in nature as we have considered the integral flight time on each
29 arc in the robust TTFP. Let E_i^l represent an edge set with the largest number of edges $(u, v) \in E_i$ from the set
30 of alternative paths P_i for flight i . $\theta_{i(u,v)}^{p_i}$ is a binary decision variable.

1
2 3.2. First-stage design decision: approach path assignment problem

3 The first-stage approach path assignment problem includes $\varphi_i^{p_i}$ and z_{jiu} ; $d(\hat{\varphi}, \hat{z})$ is the optimal
4 completion time of serving all arriving flights under the postulated uncertainty set according to a fixed-path
5 assignment solutions $\hat{\varphi}$ and \hat{z} . As mentioned earlier, the weighted path assignment in the objective function
6 (15) provides an initial solution with the least number of aeronautical holdings as a warm start in the two-stage
7 RO approach. As the objective function is to compute the completion time serving all arriving flights,
8 Constraints (6) – (10) and (13) are also included in the first-stage design decision to generate a valid lower
9 bound during convergence. The formulation of the first-stage design decision is presented as follow:

10

$$\min \sum_{i \in I} \sum_{p_i \in P_i} w_i^{p_i} \varphi_i^{p_i} + d(\hat{\varphi}, \hat{z}, \Omega) \quad (15)$$

s. t. Constraints (2) – (13)

11

12 3.3. Second-stage recourse decision: the total completion time of serving all flights in a planning horizon

13 In this section, the second-stage recourse decision computes an optimal value in the worst-case scenario
14 by realising the postulated uncertainty set Ω on the fixed path assignment solutions $\hat{\varphi}$ and \hat{z} from the first-
15 stage design decision. We consider variables C , $\tilde{\tau}_{i(u,v)}$ and $\tau_{iu}^{p_i}$ in the formulation of the second-stage recourse
16 decision. The primal form of the second stage recourse decision is presented as follow. Constraints set (17)
17 illustrates the computation of the flight time from nodes u to v under a postulated uncertainty set. The primal
18 form of the second-stage recourse decision is presented as follows:

19

$$d(\hat{\varphi}, \hat{z}, \Omega) = \max_{t \in \Omega} \min C \quad (16)$$

s. t. Constraints (6) – (10) and (13)

$$\tau_{iv}^{p_i} - \tau_{iu}^{p_i} \geq \tilde{\tau}_{i(u,v)} - M(1 - \varphi_i^{p_i}), \forall i \in I, \forall p_i \in P_i, \forall (u, v) \in E_i, u < v, \forall t \in \Omega \quad (17)$$

20

21 3.4. Benders reformulation

22 The objective function (18) of the recourse problem is presented in max-min sense and solving the primal
23 form of the second-stage recourse decision directly is complex. We, therefore, consider Benders reformulation
24 to take the dual of the inner minimisation problem in the model (6) - (10), (13), (16) and (17). Dual variables
25 $b_i^{p_i}$, $k_{iu}^{p_i}$, $a_i^{p_i}$, $g_{i(u,v)}^{p_i}$ and h_{jiu} are the multipliers of Constraints (6), (7), (8), (9), and (10), respectively, by
26 duality theory. Hence, we have Constraints (19) – (22) in the dual model. The domain of the dual variables are
27 explained in Equations (23) – (27). After applying the dual theory, the dual form of the recourse decision now
28 becomes a maximisation problem. In this regard, the realised flight time $\tilde{\tau}_{i(u,v)}$ in the primal form of model (6)
29 - (10), (13), (16) and (17) is now reformulated in form of $\underline{\tau}_{i(u,v)} + \hat{\tau}_{i(u,v)} \theta_{i(u,v)}^{p_i}$, where $\theta_{i(u,v)}^{p_i}$ is associated with

1 the Constraints (28). The dual form of the recourse decision is shown as follows:

2

$$d(\hat{\varphi}, \hat{z}, \Omega) = \max_{a,b,k,g,h} \max_{\theta} \sum_{i \in I} \sum_{p_i \in P_i} (T_i \hat{\varphi}_i^{p_i}) b_i^{p_i} + \sum_{i \in I} \sum_{p_i \in P_i} \sum_{u \in V_i} (M \hat{\varphi}_i^{p_i}) k_{iu}^{p_i} \quad (18)$$

$$+ \sum_{i \in I} \sum_{p_i \in P_i} \sum_{(u,v) \in E_i} \left(\hat{t}_{i(u,v)} + \hat{t}_{i(u,v)} \theta_{i(u,v)}^{p_i} - M(1 - \hat{\varphi}_i^{p_i}) \right) g_{i(u,v)}^{p_i}$$

$$+ \sum_{j \in I} \sum_{i, j \neq i \in I} \sum_{u \in V_j \cap V_i \setminus \{o, d\}} (S_{ji} - M(1 - \hat{z}_{jiu})) h_{jiu}$$

s. t.

$$\sum_{i \in I} \sum_{p_i \in P_i} a_i^{p_i} \leq 1 \quad (19)$$

$$b_i^{p_i} + k_{io}^{p_i} - g_{i(o, u_i^s)}^{p_i} - \sum_{j, i \neq j \in I} h_{ijo} + \sum_{j, i \neq j \in I} h_{jio} \leq 0, \forall i \in I, \forall p_i \in P_i, \forall (o, u_i^s) \in E_i \quad (20)$$

$$-a_i^{p_i} + k_{id}^{p_i} + g_{i(u_i^e, d)}^{p_i} - \sum_{j, i \neq j \in I} h_{ija} + \sum_{j, i \neq j \in I} h_{jia} \leq 0, \forall i \in I, \forall p_i \in P_i, \forall (u_i^e, d) \in E_i \quad (21)$$

$$k_{iv}^{p_i} + g_{i(u,v)}^{p_i} - g_{i(v, \pi)}^{p_i} - \sum_{j, i \neq j \in I} h_{jiv} + \sum_{j, i \neq j \in I} h_{jiv} \leq 0, \forall i \in I, \forall p_i \in P_i, \forall (u, v), (v, \pi) \in E_i, u < v, v < \pi \setminus \{o, d\} \quad (22)$$

$$b_i^{p_i} \in R^+, \forall i \in I, \forall p_i \in P_i \quad (23)$$

$$k_{iu}^{p_i} \in R^-, \forall i \in I, \forall p_i \in P_i, \forall u \in V_i \quad (24)$$

$$a_i^{p_i} \in R^+, \forall i \in I, \forall p_i \in P_i \quad (25)$$

$$g_{i(u,v)}^{p_i} \in R^+, \forall i \in I, \forall p_i \in P_i, \forall (u, v) \in E_i, u < v \quad (26)$$

$$h_{jiu} \in R^+, \forall j, i \in I, j \neq i, \forall u \in V_j \cap V_i \setminus \{o, d\} \quad (27)$$

$$\theta_{i(u,v)}^{p_i} \in \{0, 1\}, \forall i \in I, \forall p_i \in P_i, \forall (u, v) \in E_i, u < v \quad (28)$$

3

4 A linear transformation is required for the dual form of the recourse decision due to the fact that terms
5 $\hat{t}_{iuv} \theta_{i(u,v)}^{p_i} g_{i(u,v)}^{p_i}$ in (18) are nonlinear. However, the second-stage recourse decision is a disjoint bilinear

6 program over a polyhedron, where the variables θ and g are disjoint concerning different linear constraints.

7 The realised uncertain parameters θ is regulated by the Constraints (28), while the dual variables $b_i^{p_i}$, $k_{iu}^{p_i}$, $a_i^{p_i}$,

8 $g_{i(u,v)}^{p_i}$ and h_{jiu} are joint decisions by Constraints (19) – (27). We can perform a linear transformation of the

9 dual form of the model (18) – (28) by introducing an auxiliary variable $\vartheta_{i(u,v)}^{p_i}$ as shown in model (19) – (32)

10 [82, 83].

11

$$\begin{aligned}
d(\hat{\varphi}, \hat{z}, \Omega) = & \max_{a,b,k,g,h,\theta} \sum_{i \in I} \sum_{p_i \in P_i} (T_i \hat{\varphi}_i^{p_i}) b_i^{p_i} + \sum_{i \in I} \sum_{p_i \in P_i} \sum_{u \in V_i} (M \hat{\varphi}_i^{p_i}) k_{iu}^{p_i} \\
& + \sum_{i \in I} \sum_{p_i \in P_i} \sum_{(u,v) \in E_i} (\underline{t}_{iuv} - M(1 - \hat{\varphi}_i^{p_i})) g_{i(u,v)}^{p_i} + \sum_{i \in I} \sum_{p_i \in P_i} \sum_{(u,v) \in E_i} (\hat{t}_{i(u,v)}) \vartheta_{i(u,v)}^{p_i} \\
& + \sum_{j \in I} \sum_{i, j \neq i \in I} \sum_{u \in V_j \cap V_i \setminus \{o,d\}} (S_{ji} - M(1 - \hat{z}_{jiu})) h_{jiu}
\end{aligned} \tag{29}$$

s. t. Constraints (19) – (28)

$$\vartheta_{i(u,v)}^{p_i} \leq \theta_{i(u,v)}^{p_i}, \forall i \in I, \forall p_i \in P_i, \forall (u,v) \in E_i, u < v \tag{30}$$

$$\vartheta_{i(u,v)}^{p_i} \leq g_{i(u,v)}^{p_i}, \forall i \in I, \forall p_i \in P_i, \forall (u,v) \in E_i, u < v \tag{31}$$

$$\vartheta_{i(u,v)}^{p_i} \geq 0, \forall i \in I, \forall p_i \in P_i, \forall (u,v) \in E_i, u < v \tag{32}$$

1

2

4. Solution methodology

3

4

5

6

7

8

9

10

11

4.1. Benders-dual cutting plane

12

13

14

15

16

17

18

The Benders-dual cutting plane tackles the convergence procedure using strong duality in the recourse decision. Using the Objective function (29), optimality cuts can be produced to converge the two-stage RO at each iteration. The completion time of serving all arrival flights in the ζ th iteration is denoted by C^ζ . We can enumerate all extreme points of the polyhedron by Equations (34). The optimal value must be greater than or equal to C^ζ to satisfy the ζ th iteration; Λ is the set of extreme points that achieves dual information and can be obtained by solving the recourse decision until the current iteration. The optimality cut can then be generated based on the archived $\hat{b}_i^{p_i}$, $\hat{k}_{iu}^{p_i}$, $\hat{a}_i^{p_i}$, $\hat{g}_{i(u,v)}^{p_i}$ and \hat{h}_{jiu} using Equation (34).

19

20

21

22

23

24

25

The iterative procedure of the two-stage RO approach is guided by the optimal value of the First-Stage Design Decision (FSDD) and Second-Stage Recourse Decision (SSRD). ψ_{FSDD} denotes the optimal value of the FSDD with respect to the first-stage incumbent solution (φ, z) , which is the Lower Bound (LB) value in the two-stage RO approach. ψ_{SSRD} represents the optimal value of the SSRD with respect to the second-stage incumbent solution $(a, b, k, g, h, \theta | \hat{\varphi}, \hat{z}, \Omega)$, which is the Upper Bound (UB) value in the two-stage RO approach. Adding Benders-dual cuts into the relaxed first-stage design decision model, the LB value becomes a non-decreasing value along the iteration. The two-stage RO approach converge to the global optimum using

1 the iterative relaxation framework. In this regard, the termination of the iterative procedure occurs when LB
 2 value is equal to UB value. The condition $LB = UB$ also implies the robust solution is globally optimum. The
 3 pseudo code is presented in **Algorithm 1**.

4 The model of the relaxed first-stage design decision is presented as follows:

5

$$\min \sum_{i \in I} \sum_{p_i \in P_i} w_i^{p_i} \varphi_i^{p_i} + C \quad (33)$$

s. t. Constraints (2) – (5) and (11) – (12)

$$\begin{aligned} C \geq & \sum_{i \in I} \sum_{p_i \in P_i} (T_i \varphi_i^{p_i}) \hat{\delta}_i^{p_i \zeta} + \sum_{i \in I} \sum_{p_i \in P_i} \sum_{u \in V_i} (M \varphi_i^{p_i}) \hat{\kappa}_{iu}^{p_i \zeta} \\ & + \sum_{i \in I} \sum_{p_i \in P_i} \sum_{(u,v) \in E_i} (\underline{t}_{iuv} - M(1 - \varphi_i^{p_i})) \hat{g}_{i(u,v)}^{p_i \zeta} \\ & + \sum_{i \in I} \sum_{p_i \in P_i} \sum_{(u,v) \in E_i} (\hat{t}_{i(u,v)}) \theta_{i(u,v)}^{p_i} \hat{g}_{i(u,v)}^{p_i \zeta} \\ & + \sum_{j \in I} \sum_{i, j \neq i \in I} \sum_{u \in V_j \cap V_i \setminus \{o, d\}} (S_{ji} - M(1 - z_{jiu})) \hat{h}_{jiu}^{\zeta}, \forall \zeta \in \Lambda \end{aligned} \quad (34)$$

6

7 **Algorithm 1.** The pseudo code of two-stage RO approach

```

1   Set  $UB = \infty, LB = -\infty, iter = 0, CPU\_limit$ 
2   While  $Gap \geq ExitGap$  and  $CPU_{current} \leq CPU_{limit}$  do
3       Solve the relaxed first stage design decision and obtain the optimal value  $\psi_{FSDD}$ 
4        $LB \leftarrow \psi_{FSDD}$ 
5       Solve linear dual form of second stage recourse decision and obtain the optimal value  $\psi_{SSRD}$ 
6       Add optimality cut to the relaxed first stage design decision if second stage recourse decision is feasible
7       Update  $UB \leftarrow \psi_{SSRD}$ , if necessary
8       [Pareto optimality cutting plane]
9        $Gap = (UB - LB)/UB$ 
10       $iter = iter + 1$ 
11  End

```

8

9

10 4.1.1. Pareto-optimal cut by Magnanti and Wong method

11 The efficiency of the two-stage RO approach depends on the number of effective cuts, the strength of the
 12 optimality cut at each iteration and the number of iterations required to attain a global optimal value, all of
 13 which are associated with the computation time and the convergence speed of the two-stage RO approach.
 14 [Magnanti and Wong \[75\]](#) explained that the Pareto-optimal needs to be considered to determine a dominant cut
 15 in multiple optimal solutions. A proper choice of dual variables from a set of Pareto-optimal solutions is
 16 expected to enhance the convergence rate of the algorithm. [Magnanti and Wong \[75\]](#) proposed dual-variable

1 selection method to tackle the problem of different Benders cuts from multiple optimal solutions. This method
 2 tries to obtain the dual information dominates other cuts with respect to the Pareto-optimal condition.

3

4 **Definition 1.** A Pareto-optimal cut satisfies the condition that the cut is not dominated by any other cut. Dual
 5 information $(b, k, a, g$ and $h)$ represent a set of feasible values for the dual problem. A Bender cut associated
 6 with $(b^1, k^1, a^1, g^1$ and $h^1)$ dominates a cut associated with $(b^2, k^2, a^2, g^2$ and $h^2)$ on at least one point
 7 $\hat{\varphi}, \hat{z} \in X$ as explained in Equation (35) and Constraints (2) – (6), (11) and (12) hold. In this regard, it can be
 8 said that the dual information $(b^1, k^1, a^1, g^1$ and $h^1)$ dominate $(b^2, k^2, a^2, g^2$ and $h^2)$ and that can be
 9 termed as a pareto-optimal cut.

10

$$\begin{aligned}
 & \sum_{i \in I} \sum_{p_i \in P_i} (T_i \varphi_i^{p_i}) b_i^{p_i 1} + \sum_{i \in I} \sum_{p_i \in P_i} \sum_{u \in V_i} (M \varphi_i^{p_i}) k_{iu}^{p_i 1} \\
 & \quad + \sum_{i \in I} \sum_{p_i \in P_i} \sum_{(u,v) \in E_i} (\underline{t}_{i(u,v)} - M(1 - \varphi_i^{p_i})) g_{i(u,v)}^{p_i 1} \\
 & \quad + \sum_{i \in I} \sum_{p_i \in P_i} \sum_{(u,v) \in E_i} (\hat{t}_{i(u,v)}) w_{i(u,v)}^{p_i 1} \\
 & \quad + \sum_{j \in I} \sum_{i, j \neq i \in I} \sum_{u \in V_j \cap V_i \setminus \{o, d\}} (S_{ji} - M(1 - z_{jiu})) h_{jiu}^1 \\
 & \geq \sum_{i \in I} \sum_{p_i \in P_i} (T_i \varphi_i^{p_i}) b_i^{p_i 2} + \sum_{i \in I} \sum_{p_i \in P_i} \sum_{u \in V_i} (M \varphi_i^{p_i}) k_{iu}^{p_i 2} \\
 & \quad + \sum_{i \in I} \sum_{p_i \in P_i} \sum_{(u,v) \in E_i} (\underline{t}_{i(u,v)} - M(1 - \varphi_i^{p_i})) g_{i(u,v)}^{p_i 2} \\
 & \quad + \sum_{i \in I} \sum_{p_i \in P_i} \sum_{(u,v) \in E_i} (\hat{t}_{i(u,v)}) w_{i(u,v)}^{p_i 2} \\
 & \quad + \sum_{j \in I} \sum_{i, j \neq i \in I} \sum_{u \in V_j \cap V_i \setminus \{o, d\}} (S_{ji} - M(1 - z_{jiu})) h_{jiu}^2, \forall \varphi, z \in X
 \end{aligned} \tag{35}$$

11

12 A core point is required for a robust TTFP to generate a Pareto-optimal cut. The definition of a core point is
 13 given below:

14

15 **Definition 2.** A point $\varphi^0, z^0 \in X$ is a core point that exists at the region of the relative interior of the convex
 16 hull $ri(X^c)$, where $ri(\cdot)$ is the relative interior and X^c the convex hull of set X .

17

18 The core point (φ^0, z^0) is an initial fixed core point that is in accordance with [Magnanti and Wong \[75\]](#)
 19 method and the point (φ^ζ, z^ζ) of the second-stage recourse design associated to the current solution at ζ th
 20 iteration. $\Psi_{sp}(b, k, a, g, h, \theta)$ is the objective value of the second-stage recourse design associated with fixed

1 solutions φ^ζ and z^ζ . [Magnanti and Wong \[75\]](#)'s Pareto optimality cut can generate an alternative for the
 2 Pareto-optimal cut that fosters the convergence process of the two-stage RO. Model (19) – (28), (30) – (32),
 3 (36) and (37) presents the optimisation model to generate the Pareto-optimality cut by the Magnanti-Wong
 4 method.

5

$$\begin{aligned}
 \max \sum_{i \in I} \sum_{p_i \in P_i} (T_i \varphi_i^{p_i 0}) b_i^{p_i} + \sum_{i \in I} \sum_{p_i \in P_i} \sum_{u \in V_i} (M \varphi_i^{p_i 0}) k_{iu}^{p_i} \\
 + \sum_{i \in I} \sum_{p_i \in P_i} \sum_{(u,v) \in E_i} (\underline{t}_{i(u,v)} - M(1 - \varphi_i^{p_i 0})) g_{i(u,v)}^{p_i} \\
 + \sum_{i \in I} \sum_{p_i \in P_i} \sum_{(u,v) \in E_i} (\hat{t}_{i(u,v)}) w_{i(u,v)}^{p_i 0} \\
 + \sum_{j \in I} \sum_{i, j \neq i \in I} \sum_{u \in V_j \cap V_i \setminus \{o, d\}} (S_{ji} - M(1 - z_{jiu}^0)) h_{jiu}
 \end{aligned} \tag{36}$$

s. t. Constraints (19) – (28), (30) – (32)

$$\begin{aligned}
 \sum_{i \in I} \sum_{p_i \in P_i} (T_i \hat{\varphi}_i^{p_i \zeta}) b_i^{p_i} + \sum_{i \in I} \sum_{p_i \in P_i} \sum_{u \in V_i} (M \hat{\varphi}_i^{p_i \zeta}) k_{iu}^{p_i} \\
 + \sum_{i \in I} \sum_{p_i \in P_i} \sum_{(u,v) \in E_i} (\underline{t}_{i(u,v)} - M(1 - \hat{\varphi}_i^{p_i \zeta})) g_{i(u,v)}^{p_i} \\
 + \sum_{i \in I} \sum_{p_i \in P_i} \sum_{(u,v) \in E_i} (\hat{t}_{i(u,v)}) w_{i(u,v)}^{p_i} \\
 + \sum_{j \in I} \sum_{i, j \neq i \in I} \sum_{u \in V_j \cap V_i \setminus \{o, d\}} (S_{ji} - M(1 - z_{jiu}^\zeta)) h_{jiu} = \psi_{sp}(b, k, a, g, h, \theta)
 \end{aligned} \tag{37}$$

6

7

8 4.1.2. Pareto-optimal cut by Papadakos method

9 [de Sá, de Camargo and de Miranda \[77\]](#) illustrated that Constraint (35) is dense and vulnerable to
 10 numerical instability. [Papadakos \[76\]](#), therefore, developed an approximated core-point method for a Pareto-
 11 optimal cut and disregarded Constraint (37) in Magnanti-Wong method to ease the computation. Although there
 12 are several methods to obtain a core point, no practical method can guarantee a good core point according to
 13 [Mercier, Cordeau and Soumis \[84\]](#).

14

15 **Definition 3.** A core point that can provide a valid Pareto-optimal cut is equivalent to that of [Magnanti and](#)
 16 [Wong \[75\]](#) method by the model (19) – (28), (30) – (32) and (36) – (37) or [Papadakos \[76\]](#) method by (19) –
 17 (28), (30) – (32) and (36).

18

19 **Definition 4.** A point (φ^0, z^0) is a point according to [Magnanti and Wong \[75\]](#) method that exists if the feasible

1 region of the second-stage recourse decision is not empty and can span the set of projections in the first stage
 2 variables.

3 From the above definition, [Papadakos \[76\]](#) proposed an approximation-based core-point assembly method
 4 to construct an updated core point iteratively. Considerably, different core points (φ^0, z^0) may be able to
 5 generalise different pareto-optimal cuts. [Papadakos \[76\]](#) suggested that any convex combination of a valid initial
 6 point by [Magnanti and Wong \[75\]](#) method can also be a valid core point (φ^0, z^0) . An updated core point
 7 $(\varphi^{0,\zeta+1}, z^{0,\zeta+1})$ was generated by considering the convex combination of an initial core point (φ^0, z^0) and
 8 an incumbent solution (φ^ζ, z^ζ) at the ζ th iteration using Equations (38) and (39). Empirically, [Papadakos \[76\]](#)
 9 illustrated that $\lambda = 0.5$ provides the best computational efficiency in their numerical analysis.

10

$$\varphi^{0,\zeta+1} = (1 - \lambda)\varphi^0 + \lambda\varphi^\zeta \quad (38)$$

$$z^{0,\zeta+1} = (1 - \lambda)z^0 + \lambda z^\zeta \quad (39)$$

11

12 4.1.3. Proposed pareto-optimal cut by core point selection scheme λ^ζ

13 Although [Papadakos \[76\]](#) suggested that $\lambda = 0.5$ provides the best solution quality in their computational
 14 analysis, there is no guarantee that a fixed λ value will provide a good core point during an iterative process.
 15 [de Sá, de Camargo and de Miranda \[77\]](#) developed a λ -optimal method to optimise. Instead of using λ -optimal
 16 by [de Sá, de Camargo and de Miranda \[77\]](#) method at each iteration, the proposed method adjusts λ value
 17 regarding the solution quality in several iterations and gains better computational efficiency than fixed the λ
 18 value. Meta-heuristics can, somehow, be incorporated for choosing the best-incumbent λ value regarding the
 19 number of unsuccessful updates in LB for several iterations.

20 In the proposed matheuristic approach, we integrated the core components of SA proposed by [Kirkpatrick,](#)
 21 [Gelatt and Vecchi \[85\]](#), including the acceptance probabilities by the Metropolis process [\[86\]](#) and the cooling
 22 schedule. It should be noted that the best-incumbent λ value is not fixed but serves as the best value for the
 23 ζ th iteration. Therefore, λ value can change during the iterative process of the two-stage RO approach.
 24 Furthermore, the integration of the two-stage RO approach and the algorithmic components of SA rely on the
 25 interoperation and interdependence of the algorithmic framework to determine λ value. A proper best-
 26 incumbent λ value along with a stochastic process increases the possibility of generating a good core point
 27 (φ^0, z^0) and obtains a pareto-optimal cut. This incorporation on the convergence process synergies the
 28 performance of the Bender cut generation and pareto-optimal cut by λ^ζ . During the iterative process, the
 29 combinatorial cuts converge the two-stage RO problem by evaluating the incumbent LB and UB , whereas the
 30 SA determines λ value regarding the unsuccessful update on the incumbent LB at ζ th iteration. The second-
 31 stage recourse decision in the framework is equivalent to that in [Papadakos \[76\]](#) method, however, λ^ζ may
 32 change iteratively. The design of the dynamic core point λ^ζ is based on the convergence performance of LB .
 33 The number of unsuccessful change on the incumbent LB is denoted as v . This value is set to zero when the
 34 LB^ζ at the ζ th iteration is greater than $LB^{\zeta-1}$ at the $\zeta - 1$ th iteration, whereas v increase by one if LB^ζ

1 equals to $LB^{\zeta-1}$ according to Equation (40). This is an important indicator to guide the acceptance probabilities
 2 by the Metropolis process when the incumbent core point (φ^0, z^0) cannot generate a pareto-optimal cut using
 3 the incumbent solution (φ^ζ, z^ζ) at the ζ th iteration. To hold Definition 4, λ^ζ must within the range $[0, \frac{1}{2}]$
 4 according to Equation (41).

$$v = \begin{cases} v + 1 & \text{if } LB^\zeta = LB^{\zeta-1} \\ 0 & \text{if } LB^\zeta > LB^{\zeta-1} \end{cases} \quad (40)$$

$$\lambda^\zeta \in [0, \frac{1}{2}] \quad (41)$$

5 The proposed update of λ^ζ value relies on the convex combination of [Magnanti and Wong \[75\]](#) initial
 6 core point and the core point of the incumbent solution (φ^ζ, z^ζ) at the ζ th iteration. This process tries to
 7 reassemble the core point that satisfies **Definition 4** via convex combination if the incumbent point $(\varphi^{0,\zeta}, z^{0,\zeta})$
 8 does not successfully generate a strong Pareto-optimal cut in terms of the LB convergence process. The update
 9 of the λ^ζ value follows metropolis-based criteria according to Equation (42) [\[86\]](#). The value T refers to the
 10 current temperature while v can be denoted as the current temperature in the SA framework. The value v
 11 denotes the number of unsuccessful updates on LB . The increase in v results in the increase of the probabilities
 12 of the metropolis process ρ^ζ at the ζ th iteration. At this point, it can be assumed that a higher number of
 13 accumulated unsuccessful updates on LB^ζ indicates a higher chance of weaker Pareto-optimal cuts from a core
 14 point $\varphi^{0,\zeta}, z^{0,\zeta}$. Given maximum temperature T in a decreasing fashion is required to represent the annealing
 15 procedure in SA [\[85\]](#), we suggest $T^\zeta = UB^\zeta - LB^\zeta$ in our proposed matheuristic. A shrinking margin of T^ζ
 16 implies a higher chance of variation of the core point (φ^0, z^0) in the metropolis process.

$$\rho^\zeta = \frac{1}{(1 + e^{\frac{-v}{T^\zeta}})} \quad (42)$$

17 The adjustment of the λ^ζ value is based on the LB convergence process and the acceptance criterion of
 18 the metropolis process can be seen in Equation (43). At the ζ th iteration, $\lambda^{\zeta+1}$ is initially set as λ^0 ($\lambda^0 = 0.5$
 19 in our proposed model) if the current LB^ζ successfully increases after adding the Pareto-optimal cuts developed
 20 from the $\zeta - 1$ th iteration. This method tries to reset $\lambda^{\zeta+1}$ at the next iteration to reassemble a new core point
 21 $(\varphi^{0,\zeta+1}, z^{0,\zeta+1})$ similar to the method of convex combination in [Papadakos \[76\]](#) method. However, if the
 22 current LB^ζ equals $LB^{\zeta-1}$, then the Benders cut from $\zeta - 1$ th iteration is considerably weak. We attempt to
 23 reassemble the core point $(\varphi^{0,\zeta+1}, z^{0,\zeta+1})$ by linear combination of the core points at a stochastic ratio of the
 24 λ^ζ value, which is tuned by meta-heuristics. This mechanism follows the algorithmic structure of the metropolis
 25 process in SA, which considers a transition probability to adjust the λ^ζ value to diversify the core point
 26 $(\varphi^{0,\zeta+1}, z^{0,\zeta+1})$ at the next iteration. The acceptance criterion of the metropolis process of the adjustment on
 27 the λ^ζ value is determined by a random variable r , where $r = [0,1]$. If $r \geq \rho^\zeta$, then, no adjustment to the
 28 $\lambda^{\zeta+1}$ value is made. If $r < \rho^\zeta$, then the $\lambda^{\zeta+1}$ value equals $\lambda^\zeta - \Delta\lambda$. The range of λ^ζ must satisfy the condition
 29 in Equation (41). We simply set $\Delta\lambda = 0.1$ in our analysis. Indeed, a larger value of $\Delta\lambda$ implies a greater

1 amplitude of λ , and vice versa. Since [Papadakos \[76\]](#) suggested that $\lambda = 0.5$ gives the best computational
 2 performance in their analysis, we considered a minor perturbation on $\lambda^{\zeta+1}$ with $\Delta\lambda = 0.1$.

$$\lambda^{\zeta+1} = \begin{cases} \lambda^0, & \text{if } LB^\zeta > LB^{\zeta-1} \\ \lambda^\zeta, & \text{if } LB^\zeta = LB^{\zeta-1} \text{ and } r \geq \rho^\zeta \\ \lambda^\zeta - \Delta\lambda, & \text{if } LB^\zeta = LB^{\zeta-1} \text{ and } r < \rho^\zeta \end{cases} \quad (43)$$

3 At each iteration, we adopted a simple cooling strategy to govern the λ^ζ value with a constant cooling
 4 rate. The cooling scheme is suggested as $\frac{\Delta\lambda}{2}$ to maintain a balance between exploitation (diversification) and
 5 exploration (intensification). [Ng, Lee, Chan and Qin \[6\]](#) explained in the computational analysis of meta-
 6 heuristic performance that exploitation refers to the ability to search for a better solution from a promising
 7 region, while exploration refers to the ability to escape from the local optimal. The two principal performance
 8 metrics measure the tendency of the λ^ζ value through trial-and-error interactions. In our preliminary study
 9 (not shown herein to avoid lengthy computational analysis), when the cooling scheme is equivalent to $\Delta\lambda$, then
 10 the λ^ζ value is mostly equal to 0.5. The λ^ζ value tends to be 0 when we adopt $\frac{\Delta\lambda}{5}$ or $\frac{\Delta\lambda}{10}$ in the cooling scheme.
 11 We found that $\frac{\Delta\lambda}{2}$ provides a good balance in the adjustment of the λ^ζ value such that it can foster the
 12 convergence process of the two-stage RO approach. Therefore, we adopted a cooling scheme in Equation (44).

$$\lambda^{\zeta+1} = \lambda^\zeta + \frac{\Delta\lambda}{2} \quad (44)$$

13 The convex combination of a core point approximation is similar to that proposed by [Papadakos \[76\]](#). The
 14 updated core point $(\varphi^{0,\zeta+1}, z^{0,\zeta+1})$ is shown in Equations (45) and (46). As mentioned earlier, the decision of
 15 update strategy on the core point at the next iteration $(\varphi^{0,\zeta+1}, z^{0,\zeta+1})$ depends on the performance of LB^ζ and
 16 $LB^{\zeta-1}$. If the value of LB^ζ is successfully increased compared to $LB^{\zeta-1}$, the updated core point
 17 $(\varphi^{0,\zeta+1}, z^{0,\zeta+1})$ is reconstructed as the initial core point (φ^0, z^0) . Otherwise, the updated core point
 18 $(\varphi^{0,\zeta+1}, z^{0,\zeta+1})$ is a convex combination of the initial (φ^0, z^0) and incumbent core points (φ^ζ, z^ζ) using an
 19 adaptive λ^ζ .

$$\varphi^{0,\zeta+1} = \begin{cases} \varphi^0 & \text{if } LB^\zeta > LB^{\zeta-1} \\ (1 - \lambda^\zeta)\varphi^0 + \lambda^\zeta\varphi^\zeta & \text{if } LB^\zeta = LB^{\zeta-1} \end{cases} \quad (45)$$

$$z^{0,\zeta+1} = \begin{cases} z^0 & \text{if } LB^\zeta > LB^{\zeta-1} \\ (1 - \lambda^\zeta)z^0 + \lambda^\zeta z^\zeta & \text{if } LB^\zeta = LB^{\zeta-1} \end{cases} \quad (46)$$

20
 21 The pseudo code of the two-stage RO approach with the dynamic core point method by SA is presented
 22 in **Algorithm 2**.

24 **Algorithm 2.** The pseudo code of proposed two-stage RO approach with dynamic core points method by simulated annealing

```

1   Set  $UB = \infty, LB = -\infty, iter = 0, \lambda^0 = 0.5, v = 0, CPU\_limit$ 
2   Set initial core point  $(\varphi^0, z^0)$ 
3   While  $Gap \geq ExitGap$  and  $CPU_{current} \leq CPU_{limit}$  do

```

```

4      Solve the relaxed first stage design decision and obtain the optimal value  $\psi_{FSDD}$ 
5       $LB \leftarrow \psi_{FSDD}$ 
6      Solve dual form of second stage recourse decision and obtain the optimal value  $\psi_{SSRD}$ 
7      Add optimality cut to the relaxed first stage design decision if second stage recourse decision is feasible
8      IF Pareto-optimal cut is successfully obtained
      THEN
9          Add pareto-optimal cut if Papadakos model is feasible
10         Update  $UB \leftarrow \psi_{SSRD}$ , if necessary
11         IF  $LB^\zeta = LB^{\zeta-1}$ 
12             THEN  $v = v + 1$ 
13             ELSE  $v = 0$ 
14         Compute  $\rho^\zeta$  (27), where  $T^\zeta = UB^\zeta - LB^\zeta$ 
15         Update  $\lambda^\zeta$  by Equation (28), where  $r \sim U([0,1])$ 
16         Update the incumbent core point  $\varphi^{0,\zeta+1}, z^{0,\zeta+1}$  using  $\lambda^\zeta$  by (29) and (30)
17          $\lambda^{\zeta+1} = \lambda^\zeta + \frac{\Delta\lambda}{2}$ 
18          $Gap = (UB - LB)/UB$ 
19          $iter = iter + 1$ 
20     End

```

1

2 **5. Numerical study**

3 5.1. Description of the real-data instances

4 The proposed method was applied to a real-life case study in April 2018 at The Hong Kong International
5 Airport (HKIA) from a licensed API from *FlightGlobal*. We are interested in the TTFP for approaching flights
6 and a scenario that includes the largest number of flight movements at half-hour intervals. Only one set of test
7 instances on 22nd April, 2018 recorded 19 flight movements from 17:30 to 18:00. Therefore, we simply used
8 real-world instances at the HKIA on 22nd April, 2018 in our numerical analysis. The total number of approaching
9 flight movements on 22nd April, 2018 was found to be 488. The distribution of the flight movement at half-hour
10 intervals is presented in **Fig. 2**. The total number of instances is 41. The instance ID is represented by a digit
11 (hour) and one alphabet (First half-an-hour by ‘F’ or second by ‘S’) to indicate the corresponding half-hour
12 intervals of the dataset. For example, the dataset from 04:30 to 05:00 and from 23:00 to 23:30 are denoted as 4-
13 S and 23-F, respectively.

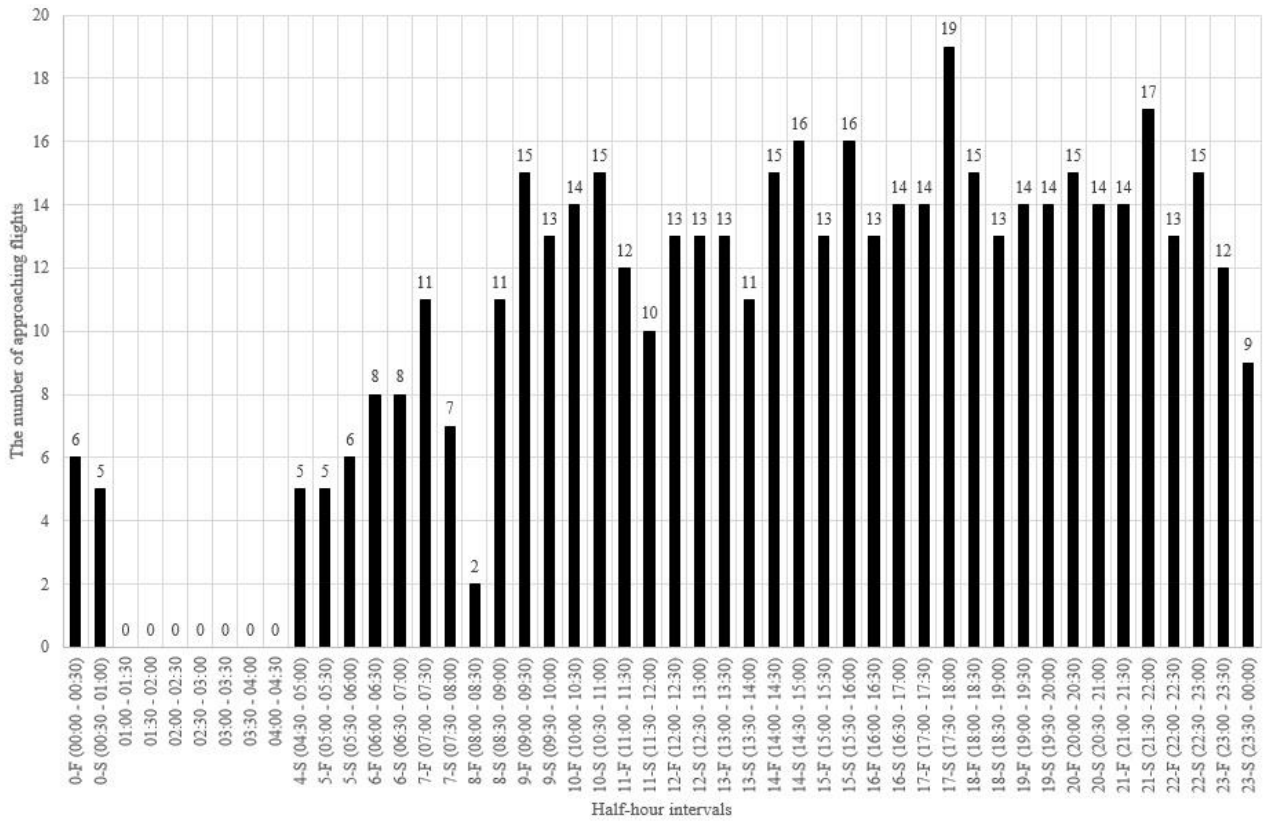


Fig. 2. The number of approaching flights at half-hour intervals on 22nd April, 2018

The arrival routes and terminal holding patterns in our model follow the terminal airspace setting in HKIA (IATA: HKG, ICAO: VHHH) as shown in Fig. 3. There are 10 entry waypoints (DOTMI, LELIM, ELATO, NOMAN, SABNO, ASOBA, DOSUT, IKELA, SIKOU and SIERA) in the HK TMA. Regarding the mono-aeronautical holding rule and the network of HK TMA, 26 alternative paths were constructed in the proposed model.

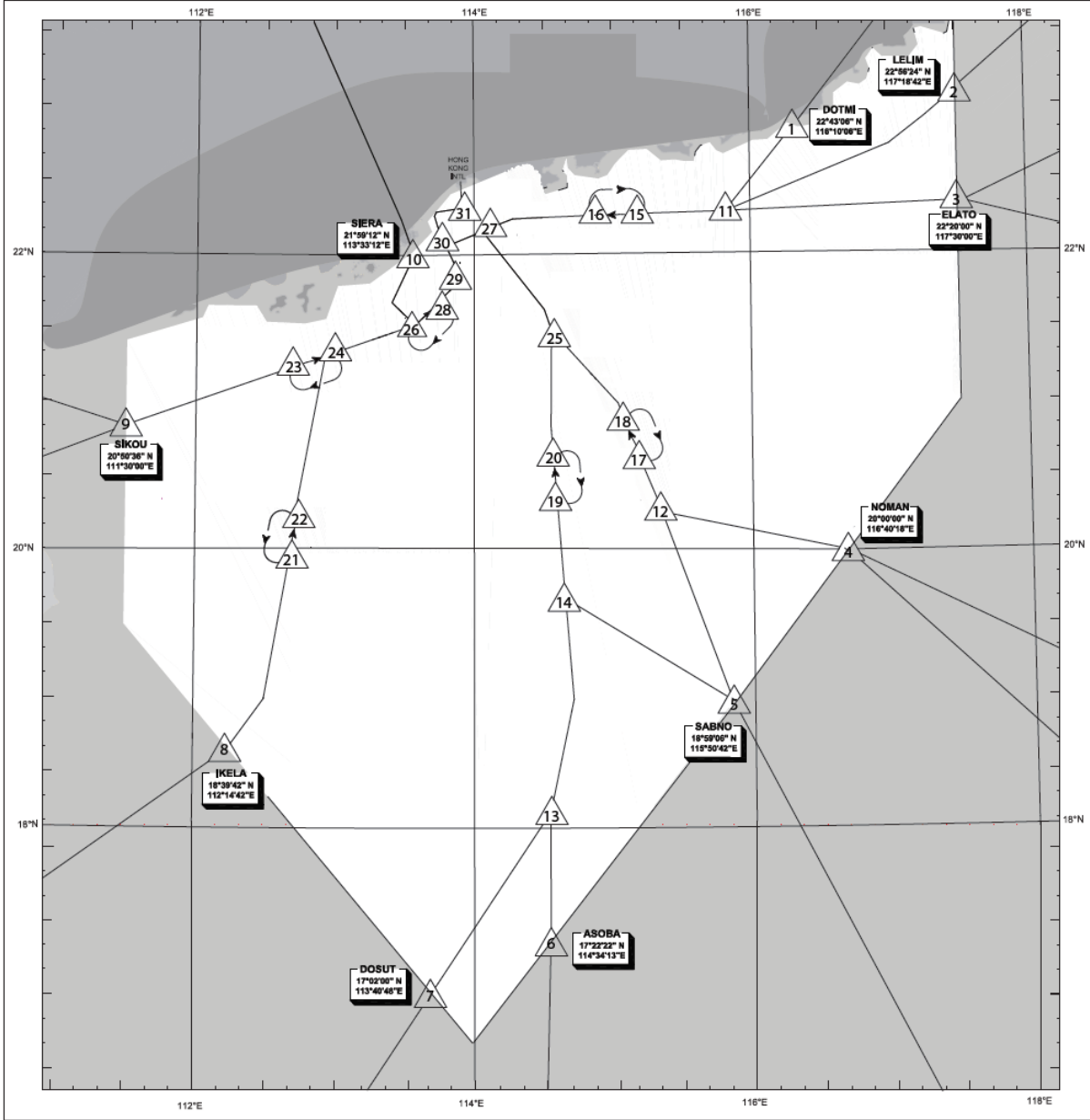


Fig. 3. The approach paths of the terminal airspace in HKIA

1
2
3
4
5
6
7
8
9
10
11
12

In the RO, the set of traversing time $\tilde{t}_{i(u,v)} \in \Omega$ is assumed to have an interval-based uncertainty $[\underline{t}_{i(u,v)}, \bar{t}_{i(u,v)}]$. The realised traversing time $\hat{t}_{i(u,v)}$ is subject to the perturbation of a normal speed profile regarding flight classes. The distance in nautical miles between waypoints is denoted as $\kappa_{(u,v)}$. The nominal traversing time $\underline{t}_{i(u,v)}$ is a flight category-based parameter that can be computed by Equation (47). The deviation from nominal $\underline{t}_{i(u,v)}$ and the realised traversing time $\bar{t}_{i(u,v)}$ can be computed by Equation (48). **Table 2** illustrates the lower bound and upper bound values of a normal speed profile under the case of an airport. **Table 3** explains the category-based longitudinal separation distance in nautical miles in HK TMA.

$$\underline{t}_{i(u,v)} = \frac{\kappa(u,v)}{\underline{\omega}_i}, \forall i \in I, \forall (u,v) \in E_i, u < v \quad (47)$$

$$\hat{t}_{i(u,v)} = \frac{\kappa(u,v)}{\underline{\omega}_i} - \frac{\kappa(u,v)}{\bar{\omega}_i}, \forall i \in I, \forall (u,v) \in E_i, u < v \quad (48)$$

1

2 **Table 2**

3 Normal speed profile regarding flight classes

<i>knots</i> ^a	<i>LSF</i>	<i>MSF</i>	<i>SSF</i>
$\underline{\omega}_i$	250	250	275
$\bar{\omega}_i$	300	270	295
$\Delta\bar{v}_i$	50	20	20

4 ^a: $v_i \text{ knots} = 3600 v_i \text{ NM/s}$, *SSF*: Small size flight; *MSF*: Medium size flight; *LSF*: Large size flight

5

6 **Table 3**

7 Longitudinal separation distance (in nautical miles)

<i>NM</i>	<i>LSF</i>	<i>MSF</i>	<i>SSF</i>
<i>LSF</i>	4	5	7
<i>MSF</i>	3	3	5
<i>SSF</i>	3	3	3

8 *SSF*: Small size flight; *MSF*: medium size flight; *LSF*: large size flight

9

10

11 5.2. Computational efficiency

12 The computation was performed using Intel Core I7 3.60GHz CPU and 16 GB RAM in a *Windows 7*
 13 *Enterprise 64-bit* operating environment. The Pareto-optimal cuts and the proposed method were coded using
 14 *C#* language with *Microsoft Visual Studio 2017* and *IBM ILOG CPLEX optimisation Studio 12.8.0*.

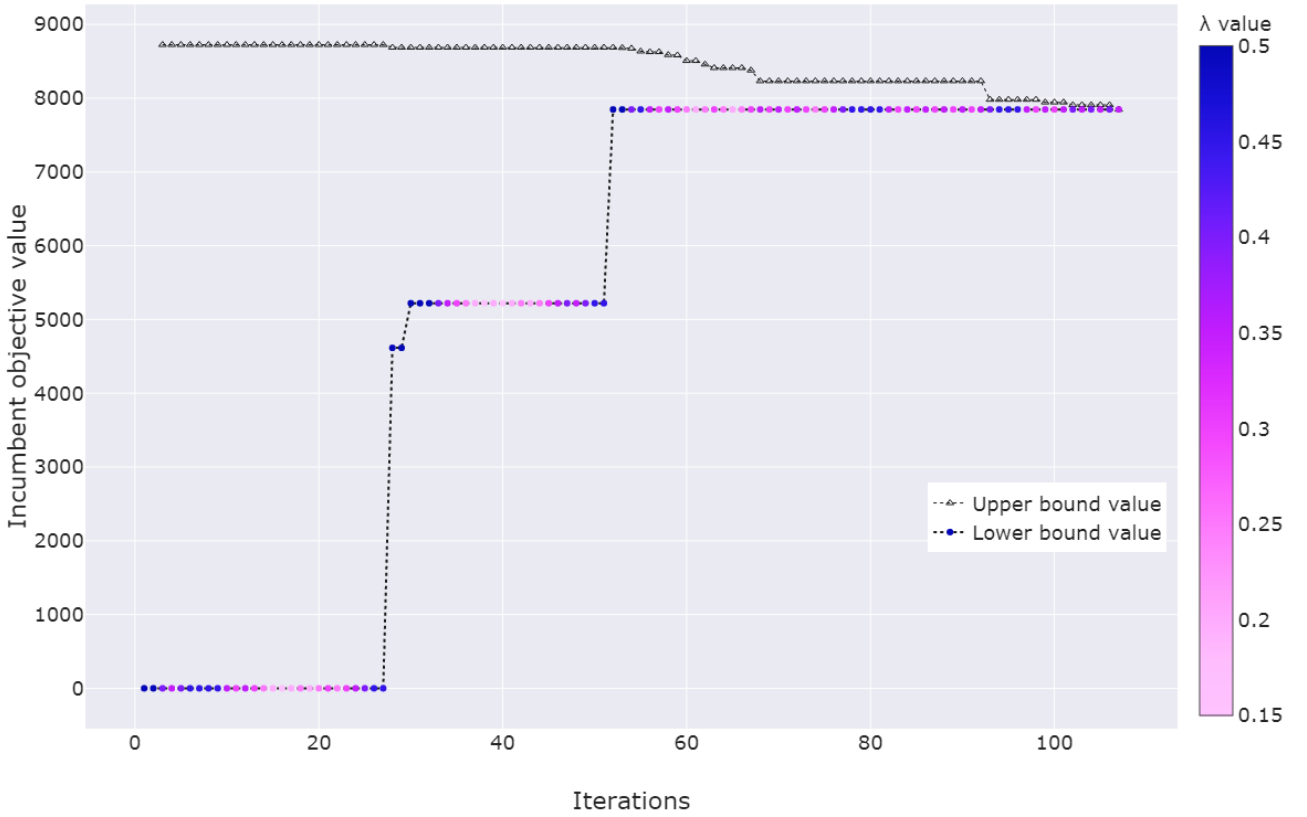
15

16 5.3. Convergence profile

17 In this section, we have provided one of the case examples from our test instance to explain the mechanism
 18 and performance of the proposed method and the overall convergence performance. Since the algorithm
 19 structure of the variants of Pareto-optimal cutting scheme differ from each other, comparison of the number of
 20 iterations may lead to biased results. We, therefore, indicate the algorithm performance using the measurement
 21 and the CPU time. Meta-heuristics do not guarantee an optimal condition and can be preserved in the form of a
 22 stochastic optimisation method. However, in our proposed approach, the optimal condition is guided by Benders
 23 dual cutting plane, duality and the iterative relaxation procedure in the two-stage RO approach. The meta-
 24 heuristics in the two-stage RO approach focuses on the core point intervention using a stochastic adjustment of
 25 the λ^ζ value. Therefore, the proposed method can guarantee an optimal solution. The stochasticity of the
 26 proposed method affects the speed of the convergence process and the CPU time.

27 The proposed algorithm performed similarly in various instances. We, therefore, select one instance to
 28 elaborate the mechanism of stochastic adjustment of the λ^ζ value in the convergence process. **Fig. 4** presents

1 the convergence process of the instance 13-S solved by the proposed method. Eleven flights were seen to enter
2 TMA from 13:30 – 14:00 in the test instance. The optimal value of the 13-S instance under the worst-case
3 scenario was 7847.23. The convergence process of the proposed method took 107 iterations to reach the
4 optimum stage. The grey plot represents the upper bound value, while the variables plot represents the lower
5 bound value. The incumbent λ^ζ value was presented using a sequential scales (from blue to pink). Dots with
6 blue colour on the lower bound curve indicates a λ^ζ value with 0.5 and dots with pink colour on the lower
7 bound curve indicates a λ^ζ value with 0. As mentioned in the section 4.1.3, λ^ζ value is adjusted with regard to
8 the convergence performance of LB value and must satisfy Constraint (26). Since a practical method is not
9 available to obtain a good core point at each iteration, the proposed method imposes stochasticity in the λ^ζ
10 value and allows reassembling the next core point $(\varphi^{0,\zeta+1}, z^{0,\zeta+1})$ from the initial (φ^0, z^0) and incumbent
11 core points (φ^ζ, z^ζ) using adaptive λ^ζ . When LB remains unchanged, the λ^ζ value has a stochastic property
12 ($\lambda^\zeta \in [0, \frac{1}{2}]$) to restructure the convex combination of the updated core point $(\varphi^{0,\zeta+1}, z^{0,\zeta+1})$. When LB is
13 successfully updated, $\lambda^{\zeta+1}$ and the updated core point are reset as its initial values (λ^ζ value with 0.5 and
14 $(\varphi^{0,\zeta+1}, z^{0,\zeta+1}) \leftarrow (\varphi^0, z^0)$).

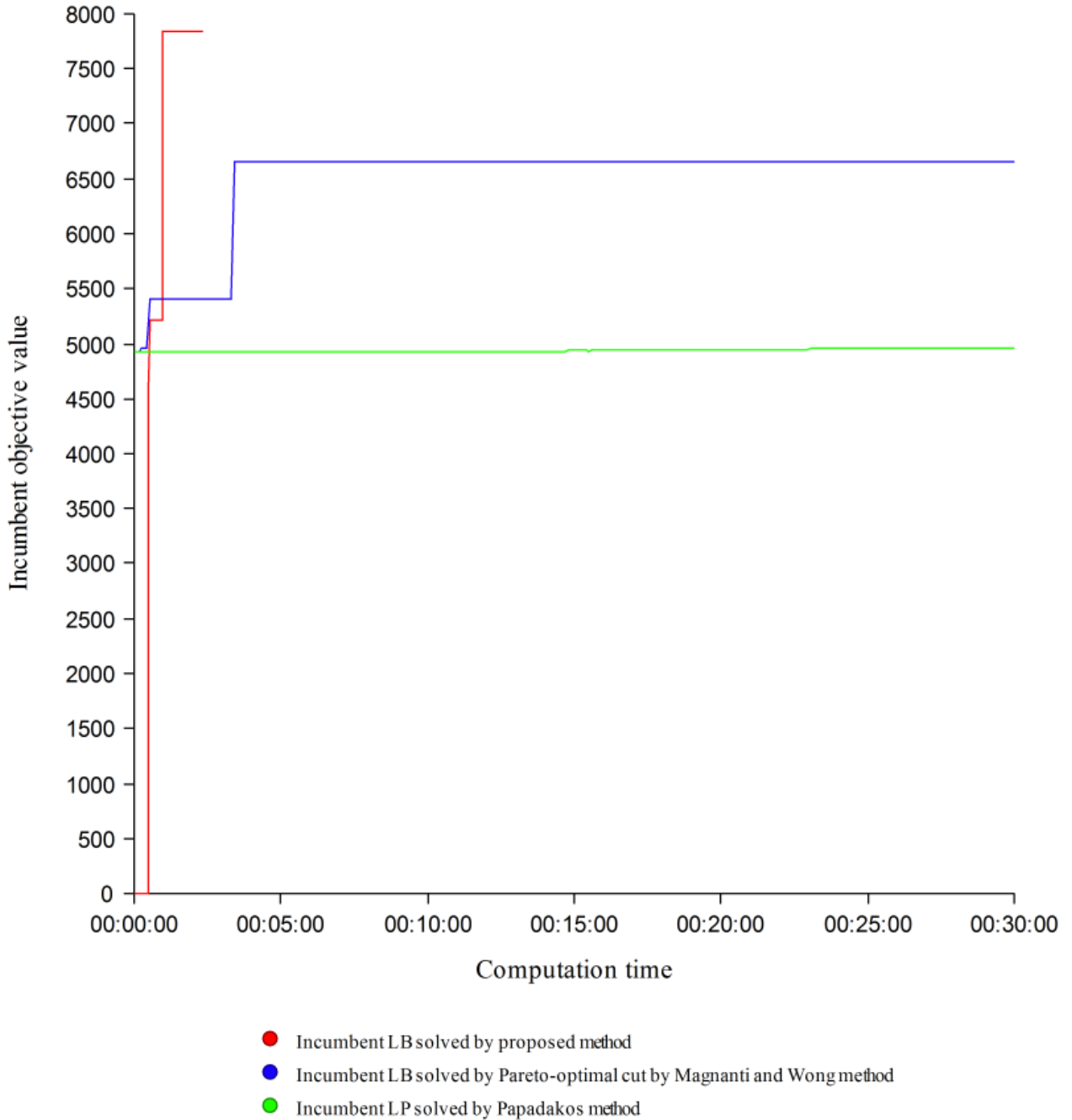


15 **Fig. 4.** Convergence process of the instance 13-S using Papadakos method with dynamic core points

16
17
18 We further map the LB performance of the two-stage RO approach, Pareto-optimal cut by Magnanti-and-
19 Wong method, Pareto-optimal cut by Papadakos method and Pareto-optimal cut by the proposed method in a
20 scatter plot with time index in **Fig. 5**. As the convergence process of the proposed method may vary in CPU

1 time, we randomly pick one result out of ten. The proposed method can reach the optimal solution and satisfy
2 the stopping criteria of the proposed method in approximately 2.5 minutes, the Pareto-optimal cut by the
3 Magnanti-and-Wong method and Papadakos method were unable to reach the optimum value at the time it
4 reached the *CPU_limit*. The results suggest that the proposed method outperforms Pareto-optimal cut by
5 Magnanti-and-Wong method and Papadakos method in solving the 13-S instance.

6



7

8

Fig. 5. The algorithms performance by solving 13-S instance regarding the incumbent lower bound value with time index

9

10

1 5.4. The efficiency of Pareto-optimal cuts

2 We measured the efficiency of the Pareto-optimal cuts through different approaches in our computational
3 analysis. The iterative process of the two-stage RO approach is terminated by either of the two conditions. (a)
4 the computational limit CPU_limit reaches 1,800 seconds or (b) the LB is greater than or equal to UB . LB
5 denotes a non-decreasing and fractional value while UB the best-known incumbent objective value. Since each
6 instance represents a half-hour interval, a CPU_limit of 1,800 seconds was chosen. The global optimal solution
7 can be obtained when LB equals UB . In this regard, we can measure the optimality gap by using Equation (49)
8 [81]. We, therefore, evaluated the algorithm performance of the variants of the Pareto-optimal cutting schemes.
9 A small value of the optimality gap indicates a close-to-optimal situation, whereas a zero value of the optimality
10 gap indicates an optimal condition.

$$Optimality\ gap\ \% (OG\%) = \frac{UB - LB}{UB} \tag{49}$$

11
12 The algorithm performance was evaluated by solving 41 real-world instances. The computational results
13 are illustrated in **Table 4**. Detailed computational results of CPU time, LB and distribution of optimality cut and
14 Pareto-optimal cut are presented in **Appendices A and B**. Since the proposed method includes randomness in
15 the convex combination of core points, we performed the analysis in 10 runtimes to measure the worst, average
16 and the best performance of the proposed method. In **Table 4**, the average optimality gap of the two-stage RO
17 approach, the two-stage RO with Magnanti-and-Wong method, two-stage RO with Papadakos method and two-
18 stage RO with the proposed dynamic core points method are 18.73%, 19.15%, 11.40% and 9.32%., respectively
19 The average CPU time of the algorithms is similar, which is in the range of 18 to 23 minutes. The results show
20 that the performance of the proposed method does not dominate the performance of other methods, since the
21 worst performance of the proposed method is slightly poor than the results from the Pareto-optimal cut by
22 Papadakos method. However, **Table 4** indicates that the average and the best performance of the proposed
23 method in 10 runtimes outperform other methods.

24

25 **Table 4**

26 Computational performance with the measurement of the optimality gap

Instance ID	# flight	Two-stage RO	Magnanti-and-Wong method	Papadakos method	Proposed method		
					Max.	Avg.	Min.
0-F	6	0.00%	0.00%	0.00%	0.00%	0.00%	0.00%
0-S	5	0.00%	0.00%	0.00%	0.00%	0.00%	0.00%
4-S	5	0.00%	0.00%	0.01%	0.01%	0.01%	0.01%
5-F	5	0.00%	0.00%	0.02%	0.02%	0.02%	0.02%
5-S	6	0.00%	0.00%	0.01%	0.01%	0.01%	0.01%
6-F	8	27.65%	0.00%	3.02%	3.62%	1.36%	0.16%
6-S	8	0.00%	25.04%	1.79%	2.68%	1.70%	0.90%
7-F	11	36.85%	38.39%	8.62%	12.95%	8.36%	6.44%
7-S	7	0.00%	0.00%	0.00%	0.00%	0.00%	0.00%

8-F	2	0.00%	0.00%	0.00%	0.00%	0.00%	0.00%
8-S	11	35.80%	35.46%	6.37%	6.39%	6.09%	5.40%
9-F	15	37.20%	37.23%	29.93%	37.50%	24.16%	7.75%
9-S	13	1.42%	36.63%	0.00%	15.72%	13.74%	0.00%
10-F	14	0.00%	0.00%	0.00%	0.00%	0.00%	0.00%
10-S	15	37.68%	37.35%	28.77%	30.78%	21.59%	8.73%
11-F	12	35.46%	35.18%	1.86%	3.85%	2.44%	0.89%
11-S	10	30.68%	0.00%	0.00%	0.00%	0.00%	0.00%
12-F	13	0.00%	0.00%	0.00%	0.05%	0.04%	0.04%
12-S	13	31.28%	30.10%	25.83%	31.38%	27.23%	17.24%
13-F	13	35.07%	35.07%	10.59%	11.36%	11.13%	10.59%
13-S	11	36.15%	18.08%	18.08%	18.15%	18.06%	17.79%
14-F	15	27.84%	28.55%	28.55%	27.10%	15.58%	7.48%
14-S	16	33.76%	33.88%	27.67%	27.67%	25.65%	7.53%
15-F	13	21.20%	20.84%	8.16%	8.16%	8.16%	8.15%
15-S	16	37.54%	37.08%	37.08%	38.14%	30.37%	0.02%
16-F	13	38.66%	39.11%	39.11%	39.64%	19.67%	0.00%
16-S	14	0.00%	0.00%	0.00%	0.00%	0.00%	0.00%
17-F	14	0.00%	38.07%	0.00%	3.49%	3.23%	2.00%
17-S	19	28.42%	29.59%	26.02%	30.56%	26.83%	25.50%
18-F	15	35.73%	0.00%	0.00%	35.73%	23.23%	0.02%
18-S	13	2.56%	0.00%	2.56%	3.22%	1.41%	0.00%
19-F	14	36.33%	36.36%	36.63%	36.05%	10.71%	7.44%
19-S	14	0.00%	0.00%	0.00%	0.00%	0.00%	0.00%
20-F	15	33.66%	34.48%	12.13%	14.21%	13.06%	10.45%
20-S	14	1.02%	34.05%	34.05%	36.45%	11.65%	1.02%
21-F	14	32.63%	32.82%	12.39%	12.41%	11.51%	5.91%
21-S	17	39.29%	39.36%	39.53%	33.14%	23.79%	17.55%
22-F	13	0.63%	0.00%	0.00%	0.63%	0.51%	0.00%
22-S	15	24.02%	22.80%	22.80%	17.68%	14.97%	11.30%
23-F	12	29.40%	29.84%	5.70%	5.72%	5.71%	5.70%
23-S	9	0.00%	0.00%	0.00%	0.01%	0.00%	0.00%
Average OG%		18.73%	19.15%	11.40%	13.28%	9.32%	4.54%
Average CPU		19:33	20:21	18:46	22:07	20:57	18:48
(mins)							

1

2

3

4

5

6

7

8

As the average OG% between the proposed algorithm and Papadakos method has about 2% difference on average. Therefore, we further conducted the statistical analysis between the benchmarking algorithms (Two-stage RO approach, Magnanti-and-Wong method and Papadakos method) and the proposed algorithm using Wilcoxon-signed ranks test. The statistical analysis was conducted with the software *IBM SPSS Statistics 22*. For the level of significance, a probable value of $\alpha = 0.05$ was considered as significant. 41 real-life case studies was evaluated and the proposed algorithm performed in 10 runtimes. The sample size of the Wilcoxon-

1 signed rank test is 410. **Table 5** presents the statistical results of Wilcoxon-signed rank test. We further evaluated
 2 the strength of the effect size by R value. The solution quality of the proposed algorithm has a greater effect
 3 than the results from the two-stage RO approach and Magnanti-and-Wong method and has a smaller effect than
 4 the results from Papadakos method. **Fig. 6** illustrates the optimality gap of algorithm performance using box
 5 diagram. The 50th percentile of the proposed method is slightly higher than the 50th percentile of the Papadakos
 6 method. However, the interquartile range of the proposed method is smaller than the benchmarking algorithms.
 7 We, therefore, conclude that the proposed algorithm statistically outperforms the benchmarking algorithms.

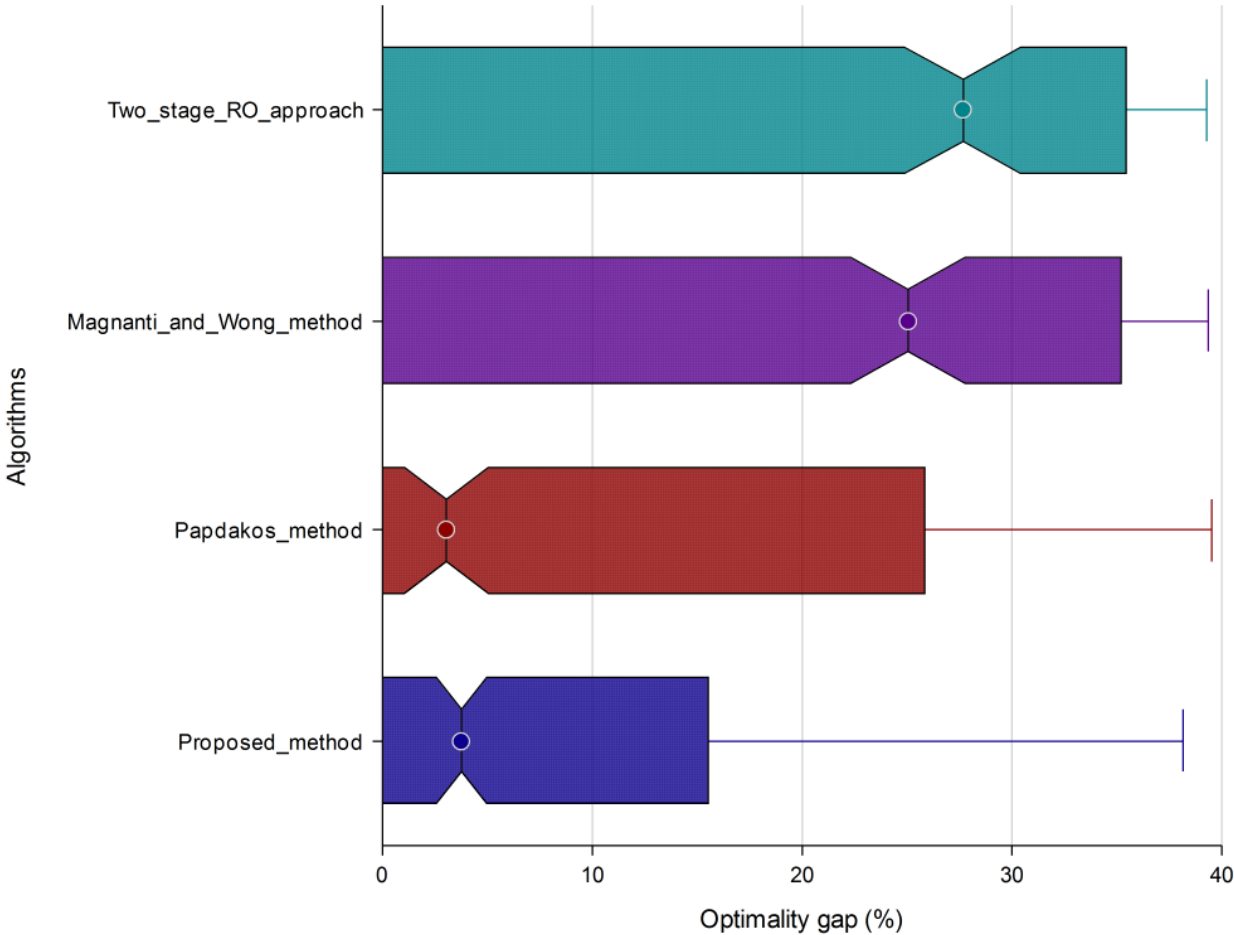
8

9 **Table 5**

10 Comparison of the benchmarking algorithms and proposed algorithm: Wilcoxon-signed ranks test

Algorithms (N = 410)	Z score	Asymp. Sig. (2 tailed)	R value	Strength of effect size
Two-stage RO	-11.582	0.000	0.5720	Large effect
Magnanti-and-Wong method	-11.295	0.000	0.5578	Large effect
Papadakos method	-2.340	0.019	0.1155	Small effect

11



12

13

14

Fig. 6. Optimality gap of different algorithms in the box plot

6. Concluding remarks

This research proposed an alternative path for the robust TTFP under uncertainty and investigated the efficiency of the variants of pareto-optimal cut and the dynamic core point selection scheme using SA algorithm. The predetermined solution for TTFP may not be applicable without the consideration of the inherent uncertainty of flight time on the approach path. The propagation of terminal traffic delays may attribute to scheduling intervention in daily operation. The RO offers a conservative approach in handling uncertainty and enhances the solution robustness resulting in a high level of solution robustness against uncertainty. The integration of the dynamic core points by SA algorithm and the two-stage RO approach by Papadakos method could enhance the efficiency of Pareto-optimal cutting scheme in solving half-hour real-world instances. The results show that the average and the best performance of the proposed method outperform the well-known Pareto-optimal cutting scheme by the Magnanti-and-Wong method and the Papadakos method in our numerical experiments.

Several interesting aspects of RO and optimisation methods can be considered for future work. These include: (a) The assumption that the terminal traffic flow model can be released in accordance with the structure of a TMA and an airport. In multiple runway systems, some runways are commonly designed solely for aircraft landing while others solely for aircraft take-off. Such a mechanism is inflexible and cannot resolve unexpected disruptive events. Pooling the available runway capacity via runway configuration switching significantly improves the robust level of runway operations and resolves the arrival-departure-demand/capacity mismatch problem. (b) Other robust criteria can also be considered in the model. Distributionally robust optimisation is a conservative approximation approach to that can estimate the expected constraint violation for possible disturbance distributions and is especially applicable under highly uncertain environments and mean-covariance information about the distributions of uncertain parameters. This optimisation offers conservative and robust runway decision-making schemes using the mean and covariance of input parameters when obtaining the probability distributions of the parameters is ambiguous or cannot be determined precisely. Investigating the risk assessment technique under the distributionally robust approach, particularly conditional-value-at-risk method, using probability distribution, described by the mean and covariance of the deviation from the predetermined landing/take-off operation time, instead of a merely known or ambiguous set of probability distributions to achieve lower-tolerance-to-loss-of-delay compensation. (c) Matheuristic is a new research direction in the research field of computational intelligence. One special challenge in the optimisation problem in airside operations is the interconnected airside activities requires real-time decisions. Many naturally inspired meta-heuristic algorithms have gained increasing popularity because of their high efficiency, which involves specific controlling parameters to maintain the balance between exploitation and exploration in the convergence process. Contrarily, the advancement of mathematical programming is still attempting to cope with the computational needs of the industry. A significant computational effort is required to resolve complex, high-dimensional and optimisation problems under uncertainty. Current research states that matheuristic is a promising optimisation technique regarding computation time and solution quality.

1 **References**

- 2 [1] K.K.H. Ng, C.K.M. Lee, F.T.S. Chan, Y. Lv, Review on meta-heuristics approaches for airside operation research,
3 Applied Soft Computing, 66 (2018) 104-133.
- 4 [2] K.K.H. Ng, C.K.M. Lee, Aircraft Scheduling Considering Discrete Airborne Delay and Holding Pattern in the Near
5 Terminal Area, in: D.-S. Huang, V. Bevilacqua, P. Premaratne, P. Gupta (Eds.) Intelligent Computing Theories and
6 Application: 13th International Conference, ICIC 2017, Springer, Liverpool, UK, 2017, pp. 567-576.
- 7 [3] Y. Qin, F.T.S. Chan, S.H. Chung, T. Qu, B. Niu, Aircraft parking stand allocation problem with safety consideration for
8 independent hangar maintenance service providers, Computers & Operations Research, 91 (2018) 225-236.
- 9 [4] D. Bertsimas, V. Goyal, On the approximability of adjustable robust convex optimization under uncertainty,
10 Mathematical Methods of Operations Research, 77 (2013) 323-343.
- 11 [5] D. Bertsimas, V. Goyal, On the power of robust solutions in two-stage stochastic and adaptive optimization problems,
12 Mathematics of Operations Research, 35 (2010) 284-305.
- 13 [6] K.K.H. Ng, C.K.M. Lee, F.T.S. Chan, Y. Qin, Robust aircraft sequencing and scheduling problem with arrival/departure
14 delay using the min-max regret approach, Transportation Research Part E: Logistics and Transportation Review, 106 (2017)
15 115-136.
- 16 [7] İ. Yanıkoğlu, B.L. Gorissen, D. den Hertog, A survey of adjustable robust optimization, European Journal of Operational
17 Research, (2018).
- 18 [8] C.K.M. Lee, K.K.H. Ng, H.K. Chan, K.L. Choy, W.C. Tai, L.S. Choi, A multi-group analysis of social media
19 engagement and loyalty constructs between full-service and low-cost carriers in Hong Kong, Journal of Air Transport
20 Management, 73 (2018) 46-57.
- 21 [9] Y. Qin, Z.X. Wang, F.T.S. Chan, S.H. Chung, T. Qu, A mathematical model and algorithms for the aircraft hangar
22 maintenance scheduling problem, Applied Mathematical Modelling, 67 (2019) 491-509.
- 23 [10] H. Aissi, C. Bazgan, D. Vanderpooten, Min-max and min-max regret versions of combinatorial optimization problems:
24 A survey, European Journal of Operational Research, 197 (2009) 427-438.
- 25 [11] A. Ben-Tal, L. El Ghaoui, A. Nemirovski, Robust optimization, Princeton University Press, 2009.
- 26 [12] H. Hu, K.K.H. Ng, Y. Qin, Robust Parallel Machine Scheduling Problem with Uncertainties and Sequence-Dependent
27 Setup Time, Scientific Programming, 2016 (2016) 13.
- 28 [13] K.K.H. Ng, M.H.M. Tang, C.K.M. Lee, Design and development of a performance evaluation system for the aircraft
29 maintenance industry, in: 2015 IEEE International Conference on Industrial Engineering and Engineering Management
30 (IEEM), IEEE, Singapore, Singapore, 2015, pp. 564-568.
- 31 [14] T. Gerz, F. Holzäpfel, D. Darracq, Commercial aircraft wake vortices, Progress in Aerospace Sciences, 38 (2002) 181-
32 208.
- 33 [15] J.A.D. Atkin, E.K. Burke, J.S. Greenwood, D. Reeson, Hybrid metaheuristics to aid runway scheduling at London
34 Heathrow airport, Transportation Science, 41 (2007) 90-106.
- 35 [16] J.A.D. Atkin, E.K. Burke, J.S. Greenwood, D. Reeson, On-line decision support for take-off runway scheduling
36 with uncertain taxi times at London Heathrow airport, Journal of Scheduling, 11 (2008) 323.
- 37 [17] J.E. Beasley, M. Krishnamoorthy, Y.M. Sharaiha, D. Abramson, Scheduling Aircraft Landings—The Static Case,
38 Transportation Science, 34 (2000) 180-197.
- 39 [18] P. Refaeilzadeh, L. Tang, H. Liu, Cross-Validation, in: L. Liu, M.T. Özsu (Eds.) Encyclopedia of Database Systems,
40 Springer US, Boston, MA, 2009, pp. 532-538.
- 41 [19] X. Hu, E.D. Paolo, Binary-Representation-Based Genetic Algorithm for Aircraft Arrival Sequencing and Scheduling,
42 IEEE Transactions on Intelligent Transportation Systems, 9 (2008) 301-310.
- 43 [20] J.E. Beasley, J. Sonander, P. Havelock, Scheduling Aircraft Landings at London Heathrow Using a Population
44 Heuristic, The Journal of the Operational Research Society, 52 (2001) 483-493.
- 45 [21] G. Bencheikh, J. Boukachour, A.E.H. Alaoui, F. Khoukhi, Hybrid method for aircraft landing scheduling based on a
46 job shop formulation, International Journal of Computer Science and Network Security, 9 (2009) 78-88.
- 47 [22] S. Capri, M. Ignaccolo, Genetic algorithms for solving the aircraft-sequencing problem: the introduction of departures
48 into the dynamic model, Journal of Air Transport Management, 10 (2004) 345-351.
- 49 [23] G. Hancerliogullari, G. Rabadi, A.H. Al-Salem, M. Kharbeche, Greedy algorithms and metaheuristics for a multiple
50 runway combined arrival-departure aircraft sequencing problem, Journal of Air Transport Management, 32 (2013) 39-48.
- 51 [24] J.V. Hansen, Genetic search methods in air traffic control, Computers & Operations Research, 31 (2004) 445-459.
- 52 [25] K.K.H. Ng, C.K.M. Lee, Makespan minimization in aircraft landing problem under congested traffic situation using
53 modified artificial bee colony algorithm, in: 2016 IEEE International Conference on Industrial Engineering and
54 Engineering Management (IEEM), IEEE, Bali, Indonesia, 2016, pp. 750-754.
- 55 [26] K.K.H. Ng, C.K.M. Lee, A modified Variable Neighborhood Search for aircraft Landing Problem, in: 2016 IEEE
56 International Conference on Management of Innovation and Technology (ICMIT), IEEE, Bangkok, Thailand, 2016, pp.
57 127-132.
- 58 [27] J.A. Bennell, M. Mesgarpour, C.N. Potts, Airport runway scheduling, 4OR, 9 (2011) 115.
- 59 [28] A. Lieder, R. Stolletz, Scheduling aircraft take-offs and landings on interdependent and heterogeneous runways,

1 Transportation Research Part E: Logistics and Transportation Review, 88 (2016) 167-188.

2 [29] A. Jacquillat, A.R. Odoni, Endogenous control of service rates in stochastic and dynamic queuing models of airport
3 congestion, *Transportation Research Part E: Logistics and Transportation Review*, 73 (2015) 133-151.

4 [30] A. Jacquillat, A.R. Odoni, M.D. Webster, Dynamic Control of Runway Configurations and of Arrival and Departure
5 Service Rates at JFK Airport Under Stochastic Queue Conditions, *Transportation Science*, 51 (2017) 155-176.

6 [31] K.K.H. Ng, C.K.M. Lee, F.T.S. Chan, A robust optimisation approach to the aircraft sequencing and scheduling
7 problem with runway configuration planning, in: *2017 IEEE International Conference on Industrial Engineering and
8 Engineering Management (IEEM)*, IEEE, Singapore, Singapore, 2017, pp. 40-44.

9 [32] K.K.H. Ng, C.K.M. Lee, F.T.S. Chan, S.Z. Zhang, Dynamic semi-mixed mode runway configuration planning and
10 runway scheduling, in: *Proceedings of International Conference on Computers and Industrial Engineering, CIE*, 2018.

11 [33] A. Jacquillat, A.R. Odoni, An Integrated Scheduling and Operations Approach to Airport Congestion Mitigation,
12 *Operations Research*, 63 (2015) 1390-1410.

13 [34] J.A. Behrends, J.M. Usher, Aircraft gate assignment: Using a deterministic approach for integrating freight movement
14 and aircraft taxiing, *Computers & Industrial Engineering*, 102 (2016) 44-57.

15 [35] J. Guépet, O. Briant, J.-P. Gayon, R. Acuna-Agost, Integration of aircraft ground movements and runway operations,
16 *Transportation Research Part E: Logistics and Transportation Review*, 104 (2017) 131-149.

17 [36] M. Samà, A. D'Ariano, P. D'Ariano, D. Pacciarelli, Optimal aircraft scheduling and routing at a terminal control area
18 during disturbances, *Transportation Research Part C: Emerging Technologies*, 47 (2014) 61-85.

19 [37] M. Samà, A. D'Ariano, F. Corman, D. Pacciarelli, Metaheuristics for efficient aircraft scheduling and re-routing at
20 busy terminal control areas, *Transportation Research Part C: Emerging Technologies*, 80 (2017) 485-511.

21 [38] M. Samà, A. D'Ariano, P. D'Ariano, D. Pacciarelli, Scheduling models for optimal aircraft traffic control at busy
22 airports: Tardiness, priorities, equity and violations considerations, *Omega*, 67 (2017) 81-98.

23 [39] M. Samà, A. D'Ariano, P. D'Ariano, D. Pacciarelli, Air traffic optimization models for aircraft delay and travel time
24 minimization in terminal control areas, *Public Transport*, 7 (2015) 321-337.

25 [40] Y. Tian, L. Wan, K. Han, B. Ye, Optimization of terminal airspace operation with environmental considerations,
26 *Transportation Research Part D: Transport and Environment*, 63 (2018) 872-889.

27 [41] L. Corolli, G. Lulli, L. Ntaimo, S. Venkatachalam, A two-stage stochastic integer programming model for air traffic
28 flow management, *IMA Journal of Management Mathematics*, 28 (2017) 19-40.

29 [42] L. El Ghaoui, F. Oustry, H. Lebret, Robust solutions to uncertain semidefinite programs, *SIAM Journal on
30 Optimization*, 9 (1998) 33-52.

31 [43] A. Ben-Tal, A. Nemirovski, Robust convex optimization, *Mathematics of operations research*, 23 (1998) 769-805.

32 [44] D. Bertsimas, M. Sim, The price of robustness, *Operations research*, 52 (2004) 35-53.

33 [45] R.L. Daniels, P. Kouvelis, Robust scheduling to hedge against processing time uncertainty in single-stage production,
34 *Management Science*, 41 (1995) 363-376.

35 [46] M.S. Lobo, Robust and convex optimization with applications in finance, in: *stanford university*, 2000.

36 [47] S. Neyshabouri, B.P. Berg, Two-stage robust optimization approach to elective surgery and downstream capacity
37 planning, *European Journal of Operational Research*, 260 (2017) 21-40.

38 [48] L. Zhao, B. Zeng, Robust unit commitment problem with demand response and wind energy, in: *2012 IEEE Power
39 and Energy Society General Meeting*, 2012, pp. 1-8.

40 [49] S. Mattia, F. Rossi, M. Servilio, S. Smriglio, Staffing and scheduling flexible call centers by two-stage robust
41 optimization, *Omega*, 72 (2017) 25-37.

42 [50] Z. Chang, S. Song, Y. Zhang, J.-Y. Ding, R. Zhang, R. Chiong, Distributionally robust single machine scheduling with
43 risk aversion, *European Journal of Operational Research*, 256 (2017) 261-274.

44 [51] Y. Wang, Y. Zhang, J. Tang, A distributionally robust optimization approach for surgery block allocation, *European
45 Journal of Operational Research*, 273 (2019) 740-753.

46 [52] L.R. Matthews, C.E. Gounaris, I.G. Kevrekidis, Designing Networks with Resiliency to Edge Failures Using Two-
47 Stage Robust Optimization, *European Journal of Operational Research*, (2019).

48 [53] L. Zhen, Y. Wu, S. Wang, Y. Hu, W. Yi, Capacitated closed-loop supply chain network design under uncertainty,
49 *Advanced Engineering Informatics*, 38 (2018) 306-315.

50 [54] S. Yan, C.-H. Tang, Inter-city bus scheduling under variable market share and uncertain market demands, *Omega*, 37
51 (2009) 178-192.

52 [55] J. He, C. Tan, Y. Zhang, Yard crane scheduling problem in a container terminal considering risk caused by uncertainty,
53 *Advanced Engineering Informatics*, 39 (2019) 14-24.

54 [56] J. Pereira, I. Averbakh, Exact and heuristic algorithms for the interval data robust assignment problem, *Computers &
55 Operations Research*, 38 (2011) 1153-1163.

56 [57] P. Kouvelis, G. Yu, Robust Scheduling Problems, in: *Robust Discrete Optimization and Its Applications*, Springer
57 US, Boston, MA, 1997, pp. 241-289.

58 [58] L.J. Basso, Airport deregulation: Effects on pricing and capacity, *International Journal of Industrial Organization*, 26
59 (2008) 1015-1031.

60 [59] D.E. Bell, Regret in Decision Making under Uncertainty, *Operations Research*, 30 (1982) 961-981.

- 1 [60] L. Marla, V. Vaze, C. Barnhart, Robust optimization: Lessons learned from aircraft routing, *Computers & Operations*
2 *Research*, 98 (2018) 165-184.
- 3 [61] T.-M. Choi, X. Wen, X. Sun, S.-H. Chung, The mean-variance approach for global supply chain risk analysis with air
4 logistics in the blockchain technology era, *Transportation Research Part E: Logistics and Transportation Review*, 127 (2019)
5 178-191.
- 6 [62] X. Wen, X. Xu, T. Choi, S. Chung, Optimal Pricing Decisions of Competing Air-Cargo-Carrier Systems--Impacts of
7 Risk Aversion, Demand, and Cost Uncertainties, *IEEE Transactions on Systems, Man, and Cybernetics: Systems*, (2019)
8 1-15.
- 9 [63] N. Pyrgiotis, K.M. Malone, A. Odoni, Modelling delay propagation within an airport network, *Transportation Research*
10 *Part C: Emerging Technologies*, 27 (2013) 60-75.
- 11 [64] C.-L. Wu, K. Law, Modelling the delay propagation effects of multiple resource connections in an airline network
12 using a Bayesian network model, *Transportation Research Part E: Logistics and Transportation Review*, 122 (2019) 62-77.
- 13 [65] P. Fleurquin, J.J. Ramasco, V.M. Eguiluz, Systemic delay propagation in the US airport network, *Scientific Reports*,
14 3 (2013) 1159.
- 15 [66] B.L. Gorissen, D. den Hertog, Robust nonlinear optimization via the dual, *Optimization Online*, (2015).
- 16 [67] A. Beck, A. Ben-Tal, Duality in robust optimization: primal worst equals dual best, *Operations Research Letters*, 37
17 (2009) 1-6.
- 18 [68] A. Khan Waqar, C. S., M. Awan, X. Wen, Machine learning facilitated business intelligence (Part I): Neural networks
19 learning algorithms and applications, *Industrial Management & Data Systems*, ahead-of-print (2019).
- 20 [69] X. Wen, T. Siqin, How do product quality uncertainties affect the sharing economy platforms with risk considerations?
21 A mean-variance analysis, *International Journal of Production Economics*, (2019) 107544.
- 22 [70] B.L. Gorissen, İ. Yanıkoğlu, D. den Hertog, A practical guide to robust optimization, *Omega*, 53 (2015) 124-137.
- 23 [71] İ. Yanıkoğlu, B.L. Gorissen, D. den Hertog, A survey of adjustable robust optimization, *European Journal of*
24 *Operational Research*, 277 (2019) 799-813.
- 25 [72] C. Lei, W.-H. Lin, L. Miao, A two-stage robust optimization approach for the mobile facility fleet sizing and routing
26 problem under uncertainty, *Computers & Operations Research*, 67 (2016) 75-89.
- 27 [73] R. Rahmaniani, T.G. Crainic, M. Gendreau, W. Rei, The Benders decomposition algorithm: A literature review,
28 *European Journal of Operational Research*, 259 (2017) 801-817.
- 29 [74] T.L. Magnanti, R.W. Simpson, Transportation network analysis and decomposition methods, in, United States. Dept.
30 of Transportation. Research and Special Programs ..., 1978.
- 31 [75] T.L. Magnanti, R.T. Wong, Accelerating Benders decomposition: Algorithmic enhancement and model selection
32 criteria, *Operations research*, 29 (1981) 464-484.
- 33 [76] N. Papadakos, Practical enhancements to the Magnanti-Wong method, *Operations Research Letters*, 36 (2008) 444-
34 449.
- 35 [77] E.M. de Sá, R.S. de Camargo, G. de Miranda, An improved Benders decomposition algorithm for the tree of hubs
36 location problem, *European Journal of Operational Research*, 226 (2013) 185-202.
- 37 [78] K.K.H. Ng, C.K.M. Lee, S.Z. Zhang, K. Wu, W. Ho, A multiple colonies artificial bee colony algorithm for a
38 capacitated vehicle routing problem and re-routing strategies under time-dependent traffic congestion, *Computers &*
39 *Industrial Engineering*, 109 (2017) 151-168.
- 40 [79] H. Zhang, L. Tang, C. Yang, S. Lan, Locating electric vehicle charging stations with service capacity using the
41 improved whale optimization algorithm, *Advanced Engineering Informatics*, 41 (2019) 100901.
- 42 [80] F. Ballestín, R. Leus, Resource-Constrained Project Scheduling for Timely Project Completion with Stochastic
43 Activity Durations, *Production and Operations Management*, 18 (2009) 459-474.
- 44 [81] M.E. Bruni, L. Di Puglia Pugliese, P. Beraldi, F. Guerriero, An adjustable robust optimization model for the resource-
45 constrained project scheduling problem with uncertain activity durations, *Omega*, 71 (2017) 66-84.
- 46 [82] R. Horst, H. Tuy, *Global optimization: Deterministic approaches*, Springer Science & Business Media, 2013.
- 47 [83] R. Montemanni, L.M. Gambardella, The robust shortest path problem with interval data via Benders decomposition,
48 *4OR*, 3 (2005) 315-328.
- 49 [84] A. Mercier, J.-F. Cordeau, F. Soumis, A computational study of Benders decomposition for the integrated aircraft
50 routing and crew scheduling problem, *Computers & Operations Research*, 32 (2005) 1451-1476.
- 51 [85] S. Kirkpatrick, C.D. Gelatt, M.P. Vecchi, Optimization by simulated annealing, *science*, 220 (1983) 671-680.
- 52 [86] N. Metropolis, A.W. Rosenbluth, M.N. Rosenbluth, A.H. Teller, E. Teller, Equation of state calculations by fast
53 computing machines, *The journal of chemical physics*, 21 (1953) 1087-1092.
- 54